Ecological Modelling 384 (2018) 353–369

Contents lists available at ScienceDirect

Ecological Modelling

journal homepage: www.elsevier.com/locate/ecolmodel

Assessing timber volume recovery after disturbance in tropical forests – A new modelling framework

Camille Piponiot[a,b,c,*], Géraldine Derroire[b], Laurent Descroix[d], Lucas Mazzei[e], Ervan Rutishauser[f,g], Plinio Sist[h], Bruno Hérault[h,i,**]

[a] Université de Guyane, UMR EcoFoG (AgroParistech, Cirad, CNRS, Inra, Université des Antilles), Campus Agronomique, Kourou, French Guiana
[b] Cirad, UMR EcoFoG (AgroParistech, CNRS, Inra, Université des Antilles, Université de la Guyane), Campus Agronomique, Kourou, French Guiana
[c] CNRS, UMR EcoFoG (AgroParistech, Cirad, Inra, Université des Antilles, Université de la Guyane), Campus Agronomique, Kourou, French Guiana
[d] ONF-Guyane, Réserve de Montabo, 97307 Cayenne, French Guiana
[e] Embrapa Amazônia Oriental, Belém, Brazil
[f] CarboForExpert, Geneva, Switzerland
[g] Smithsonian Tropical Research Institute, Gamboa, Panama
[h] Cirad, Univ Montpellier, UR Forests and Societies, Montpellier, France
[i] INPHB (Institut National Polytechnique Félix Houphouet Boigny), Yamoussoukro, Cote d'Ivoire

ARTICLE INFO

Keywords:
Disturbance
Recovery
Tropical forest management
Sustainability
Ecosystem modelling

ABSTRACT

One third of contemporary tropical forests is designated by national forest services for timber production. Tropical forests are also increasingly affected by anthropogenic disturbances. However, there is still much uncertainty around the capacity of tropical forests to recover their timber volume after logging as well as other disturbances such as fires, large blow-downs and extreme droughts, and thus on the long-term sustainability of logging.

We developed an original Bayesian hierarchical model of Volume Dynamics with Differential Equations (VDDE) to infer the dynamic of timber volumes as the result of two ecosystem processes: volume gains from tree growth and volume losses from tree mortality. Both processes are expressed as explicit functions of the forest maturity, *i.e.* the overall successional stage of the forest that primarily depends on the frequency and severity of the disturbances that the forest has undergone. As a case study, the VDDE model was calibrated with data from Paracou, a long-term disturbance experiment in a neotropical forest where over 56 ha of permanent forest plots were logged with different intensities and censused for 31 years. With this model, we could predict timber recovery at Paracou at the end of a cutting cycle depending on the logging intensity, the rotation cycle length, and the proportion of commercial volume.

The VDDE modelling framework developed presents three main advantages: (i) it can be calibrated with large tree inventories which are widely available from national forest inventories or logging concession management plans and are easy to measure, both on the field and with remote sensing; (ii) it depends on only a few input parameters, which can be an advantage in tropical regions where data availability is scarce; (iii) the modelling framework is flexible enough to explicitly include the effect of other types of disturbances (both natural and anthropogenic: e.g. blow-downs, fires and climate change) on the forest maturity, and thus to predict future timber provision in the tropics in a context of global changes.

1. Introduction

Tropical forests are increasingly prone to anthropogenic disturbances: in 2017, only 20% of the remaining tropical forests were considered as undisturbed and structurally intact (Potapov et al., 2017), and this proportion is likely to decrease under future human pressure (Lewis et al., 2015). Disturbances, here defined as occasional events provoking sharp biomass losses (Rykiel, 1985), alter forest structure, notably average tree height (Tyukavina et al., 2016; Rutishauser et al., 2016), thus decreasing in turn carbon and timber stocks (Espírito-Santo et al., 2014). Human activities are increasing the frequency and severity of disturbances in tropical forests, both directly (e.g. through logging

* Corresponding author at: Université de la Guyane, UMR EcoFoG (AgroParistech, Cirad, CNRS, Inra, Université des Antilles), Campus Agronomique, 97310 Kourou, French Guiana.
** Corresponding author at: Cirad, UR Forests and Societies, Campus International de Baillarguet, 34398 Montpellier, Cedex 5, France.
E-mail addresses: camille.piponiot@gmail.com (C. Piponiot), bruno.herault@cirad.fr (B. Hérault).

https://doi.org/10.1016/j.ecolmodel.2018.05.023
Received 8 December 2017; Received in revised form 25 May 2018; Accepted 27 May 2018
Available online 18 July 2018
0304-3800/

and fires (Potapov et al., 2017)) and indirectly (e.g. through climate change and forest fragmentation (Laurance and Williamson, 2001)). In this context, assessing the effect of disturbances on the recovery of tropical forests is of paramount importance to better estimate future timber provision. The latter is predominantly done through selective logging that consists in harvesting a few high-value tree species and leaving the rest of the forest to natural recovery. Such forest management is widespread: it has been estimated that between 2005 and 2010, more than 50% of carbon emissions from tropical forest degradation were caused by selective logging (Pearson et al., 2017) and 425 Mha (c. 30% of the world wet tropical forests) are currently intended for timber production by National Forest Services (Blaser et al., 2011; Pan et al., 2013).

Though most of the forest cover is maintained after selective logging, typically 50–90% (Asner et al., 2002; Cannon et al., 1994; Laporte et al., 2007), opening the forest and felling trees has deep environmental consequences, such as an obvious reduction of timber stocks (Keller et al., 2004), but also large carbon emissions due to wood harvest and incidental mortality (Pearson et al., 2014), modification of tree species composition (de Avila et al., 2015) or fauna diversity (Burivalova et al., 2014). In the absence of subsequent disturbances (*e.g.* clear-cutting, fire, new logging events), the forest naturally regenerates and recovers at least part of its ecosystem values (e.g. carbon and timber stocks Piponiot et al., 2016a,b; Rutishauser et al., 2015; Blanc et al., 2009), before being selectively logged again. With logging rotation generally ranging between 20 and 30 years (Blaser et al., 2011), such cutting cycle duration may be sufficient to recover C stocks but not the volume of commercial species (Rutishauser et al., 2015; Roopsind et al., 2017) leading to unsustainable wood production on the long run.

There has been a strong debate over the past two decades on the role of selective logging in production forests as a tool for tropical forest conservation (Rice et al., 1997; Bawa and Seidler, 1998; Putz et al., 2001; Edwards et al., 2014). If logged forests are to be considered as a piece of an integrative conservation scheme, they should at least retain most of their environmental and economical values in time: this is the main challenge for modern tropical forest management. Sustainable forest management is indeed defined by the International Tropical Timber Organisation as "*the process of managing forest to achieve one or more clearly specified objectives of management […] without undue reduction of its inherent values and future productivity and without undue undesirable effects on the physical and social environment*" (ITTO, 1992). Due to the social and economical benefits it brings, sustainable timber harvest is even considered to be an efficient tool that gives additional value to forests that would else be cleared for agriculture (Edwards et al., 2014). One of the cornerstone of sustainability in forest management is the maintenance of high productivity (ITTO, 1992) to allow the recovery of timber stocks at the end of a cutting cycle. This is a critical point as in most selectively logged forests, this criterion is not achieved and many studies report a drop in total volume at the end of the first cutting cycle (Putz et al., 2012).

Previous studies simulating post-logging timber recovery have made large uses of individual-based models (Huth and Ditzer, 2001; Kammesheidt et al., 2001; Valle et al., 2007; Sebbenn et al., 2008) or transition matrix models (Macpherson et al., 2010; Gourlet-Fleury et al., 2005a,b). Such models perform well at locally predicting forest dynamics (Liang and Picard, 2013), but their high level of complexity and data requirements make the understanding of emergent patterns uneasy (Grimm, 2005). Furthermore, recruitment of small trees is a key process for long-term prediction in transition matrix models as well as in individual-based models (Liang and Picard, 2013; Berger et al., 2008; Fischer et al., 2016) and requires data from permanent sample plots with measurements of trees from relatively low size classes, typically above 10 cm of Diameter at Breast Height (DBH) or less (Gourlet-Fleury et al., 2005a,b; Phillips et al., 2004). Because small trees are particularly numerous in tropical forests, measuring them is costly (Picard et al., 2010; Kiyono et al., 2011): for example it takes approximately 10–15 times longer to measure all trees above 10 cm DBH than only trees above 50 cm DBH (Alder and Synnott, 1992). In this context, high-quality data coming from long-running permanent sample plots remain scarce in the tropics, hampering large-scale modelling of forest dynamics that would feed forest management plans with robust productivity predictions (Picard et al., 2010).

On the other side of the spectrum, coarse scale models such as Dynamic Global Vegetation Models (DGVM; e.g. LPJ-DGVM Sitch et al., 2003) allow efficient large-scale forest dynamics prediction with little input data, relying on a wide set of mechanistic assumptions. These models were initially developed to simulate ecosystem carbon fluxes, but can be used to predict volume dynamics when coupled with individual-based models (e.g. SEIB-DGVM Sato et al., 2007). Nevertheless DGVMs generally adopt a top-down approach, and are thus not fit to integrate field data such as inventory data, that are merely used for validation. As a consequence DGVMs can sometimes have conflicting results and poorly predict observed regional patterns of carbon dynamics (Johnson et al., 2016).

In this study, we propose an original model of Volume Dynamics with Differential Equations (VDDE) to assess total volume stocks and recovery based on forest inventory data. Instead of using detailed information (*i.e.* all trees) to model all demographic process (*i.e.* recruitment, growth and mortality) with great precision, we deliberately chose to favour model simplicity and rely upon broadly available data, *i.e.* the volume of all trees above 50 cm DBH (the official minimum cutting DBH in most tropical countries Blaser et al., 2011) hereinafter referred to as total volume. The VDDE model was developed and calibrated with data from the Paracou research station, a long-term large-scale disturbance experiment in Amazonia, where 56 ha of tropical forest have been monitored for 30 years after being disturbed (selective logging, poison girdling, fuelwood harvesting).

Anthropogenic or natural disturbances, such as logging or droughts, affect forests as a whole and induce a shift in forest functioning (Hérault and Piponiot, 2018). Even though the return frequency of these episodic succession-inducing events is not well known, this abrupt disturbance – slow recovery has long been described in tropical forests, as well as in temperate and boreal forests (Frolking et al., 2009; Liu et al., 2011; Chambers et al., 2013). Our assumption is that both the volume gain and the volume loss from mortality (hereinafter referred to as volume mortality) inherently depend on the overall successional stage of a forest (Rödig et al., 2018; Volkova et al., 2018), hereinafter referred to as forest maturity. While at our study site, a limited number of disturbances (selective logging, poison girdling and fuelwood harvesting) were experienced, tropical forests may undergo many other forms of anthropogenic and natural disturbances, such as droughts or fires that, similarly to logging, are associated with over-mortality that can drastically decrease trees > 50 cm DBH volume. Their effect on the forest volume dynamics can thus be modelled within the VDDE framework as a decrease in the forest maturity.

2. Methods

2.1. Study site

The study is based on data from Paracou research station (5°18′ N, 52°55′ W), a long-term large-scale disturbance experiment located in a lowland tropical forest in French Guiana (Gourlet-Fleury et al., 2004). The climate is affected by the north/south movements of the Inter-Tropical Convergence Zone and the site receives nearly two-thirds of its annual 3041 mm of precipitation between mid-March and mid-June, and less than 50 mm per month in September and October (Wagner et al., 2011). The forest composition is typical of the Guyana Shield rainforests (ter Steege et al., 2013), dominated by Chrysobalanaceae, Fabaceae and Lecythidaceae, and with approximately 180 species of trees ≥10 cm DBH per ha. 12 permanent forest plots (75 ha total) were

monitored for 31 year (from 1984 to 2015). 9 plots (56.25 ha total) of the 12 plots underwent different logging treatments from 1986 to 1988: (i) 3 plots were selectively logged in 1986, causing a median volume loss of 34.1 m^3 (95% credibility interval: 24.4–62.0 $m^3\,ha^{-1}$); (ii) 6 were selectively logged in 1986 and were then applied timber stand improvement from 1987 to 1988; treatment-induced over-mortality in those plots lasted until 1990, causing a median volume loss of 90.1 $m^3\,ha^{-1}$ (95% credibility interval: 52.4–138.3 $m^3\,ha^{-1}$).

2.2. Measurements and volume computation

In all plots all trees ≥10 cm DBH were identified, tagged and mapped, and had their DBH measured every year between 1984 and 1995 and every 2 years since then (1997–2015). The volume $V_{i,p,k}$ (m^3) of each tree i in plot p at census $k \geq 1$ was calculated using a locally calibrated equation (Guitet et al., 2016) currently used by the National Forest Service:

$$\forall\, i \in I_{p,k},\ V_{i,p,k} = -0.035829 + 8.7634 \times \mathrm{DBH}^2_{i,p,k} \tag{1}$$

where $I_{p,k}$ is the set of live trees ≥50 cm DBH in plot p at census k and $DBH_{i,p,k}$ is the diameter at breast height (in m) of the tree i at census k. The total volume ($m^3\,ha^{-1}$) of plot p, with a total area $Surf_p$ (ha), at census k is thus:

$$V_{p,k} = \sum_{i \in I_{p,k}} V_{i,p,k} \times (\mathrm{Surf}_p)^{-1} \tag{2}$$

Annual volume gain $\Delta Vg_{p,k}$ and annual volume mortality $\Delta Vm_{p,k}$ ($m^3\,ha^{-1}\,yr^{-1}$) were computed as:

$$\forall\, k \geq 2,\ \begin{cases} \Delta \mathrm{Vg}_{p,k} = \sum_{i \in I_{p,k}} (V_{i,p,k} - V_{i,p,k-1}) \times [\Delta t_k \times \mathrm{Surf}_p]^{-1} \\ \Delta \mathrm{Vm}_{p,k} = \sum_{i \in I_{p,k-1} \cap \overline{I_{p,k}}} (V_{i,p,k} - V_{i,p,k-1}) \times [\Delta t_k \times \mathrm{Surf}_p]^{-1} \end{cases} \tag{3}$$

where $I_{p,k}$ is the set of live trees ≥50 cm DBH in plot p at census k and $I_{p,k-1} \cap \overline{I_{p,k}}$ is the set of trees that died between censuses $k-1$ and k in plot p. If a given tree $i \in I_{p,k}$ was < 50 cm DBH at census $k-1$, then $V_{i,p,k-1} = 0$, and Δt_k is the time interval between censuses k and $k-1$.

The commercial volume, *i.e.* the volume of merchantable trees, was computed as the sum of all trees from species that were effectively logged in Paracou at the time of the experiment. The list of logged species in Paracou is provided in Table E2.

2.3. Conceptual framework

Forest maturity. In the newly developed VDDE model presented here, the dynamic of total volume is the result of two ecosystem processes: volume gains from tree growth and volume losses from tree mortality (Fig. 1). These processes are both expressed as functions of forest maturity. Forest maturity is a hidden variable of the VDDE model that gradually increases over time until a new disturbance, either natural (e.g. large blow-down) or human-induced (e.g. logging), occurs and abruptly decreases forest maturity (see Fig. 2). To capture the disturbance-recovery dynamic, we define the forest maturity as the time it would take for a given forest stand to grow from scratch and reach its current state in the absence of major disturbances. The forest maturity is thus expressed in a time-equivalent measure (for example in years). By definition, the maturity and total volume are null when no tree has reached 50 cm DBH (not observed in our data).

Let us consider the theoretical case where the forest recovers from scratch and is not subject to any disturbance. Let t be the maturity of the stand, in years: $V(t=0) = 0$ and $\forall t > 0$, $V(t) > 0$, with $V(t)$ the total volume of the stand at maturity t. The total volume change is modelled as:

$$\frac{\mathrm{dV}(t)}{\mathrm{dt}} = g(t) - m(t) \tag{4}$$

The volume gain from growth $g(t)$ is the stand annual volume productivity. By analogy with carbon sequestration in plants (Malhi, 2012), we consider this net volume productivity to be the difference of gross volume productivity $GVP(t)$ and the volume loss due to respiration $VR(t)$.

The gross volume productivity GVP increases with forest maturity until reaching a finite limit, the maximum gross productivity α_G:

$$\mathrm{GVP}(t) = \alpha_G \times (1 - e^{-\beta_G \times t}) \tag{5}$$

where β_G is the rate at which the asymptotic state is reached. Note that $GVP(t)$ increases with forest maturity and decelerates when approaching maximum gross productivity.

The respiration VR, *i.e.* the energy cost of maintenance, is proportional to the total volume:

$$\mathrm{VR}(t) = \theta \times V(t) \tag{6}$$

where θ is a constant. Note that $VR(t)$ is assumed to increase linearly with total volume.

The net volume productivity is given by the difference of $GVP(t)$ and $VR(t)$, resulting in a hump-shaped curve (Fig. 3), similar to previous results from forest carbon cycle (Chen et al., 2002; He et al., 2012; Volkova et al., 2018).

We expect the annual volume mortality to reach in time a finite limit α_M at a rate β_M. We thus have:

$$\forall\, t > 0,\ \begin{cases} g(t) = \mathrm{GVP}(t) - \mathrm{VR}(t) = \alpha_G \times (1 - e^{-\beta_G t}) - \theta \times V(t) \\ m(t) = \alpha_M \times (1 - e^{-\beta_M t}) \\ \frac{\mathrm{dV}(t)}{\mathrm{dt}} = g(t) - m(t) \end{cases} \tag{7}$$

We get the non-homogeneous differential equation of 1st order:

$$\begin{cases} \frac{\mathrm{dV}(t)}{\mathrm{dt}} = \alpha_G \times (1 - e^{-\beta_G t}) - \theta \times V(t) - \alpha_M \times (1 - e^{-\beta_M t}) \\ \text{with } V(0) = 0 \end{cases} \tag{8}$$

The solution of this equation is:

$$V(t) = \frac{\alpha_G}{\theta}\left(1 - \frac{\theta \times e^{-\beta_G t} - \beta_G \times e^{-\theta t}}{\theta - \beta_G}\right) - \frac{\alpha_M}{\theta}\left(1 - \frac{\theta \times e^{-\beta_M t} - \beta_M \times e^{-\theta t}}{\theta - \beta_M}\right) \tag{9}$$

To have $\forall t \geq 0$, $V(t) \geq 0$, we must have $\alpha_G \geq \alpha_M$ and $\beta_M \geq \beta_G \times \frac{\alpha_G}{\alpha_M}$.

We thus have the following equations:

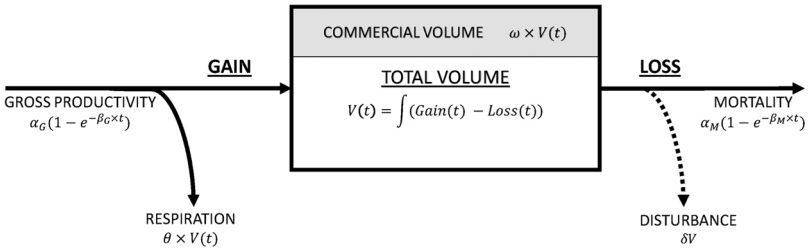

Fig. 1. Diagram of the main components of the VDDE model. The measured quantities are underlined. Solid arrows represent annual volume changes, the dashed arrow represents an *occasional* volume change, and the box represents the volume stock. Values of volume changes and stocks at a given forest maturity t are given by the equations, with the following parameters: α_G and α_M the gross volume productivity and mortality (resp.) of an infinitely mature stand and β_G, β_M the respective rate at which these values are reached; θ the volume respiration rate; ω the proportion of commercial volume; δV the volume loss caused by a given disturbance. Parameters posterior distributions are given in Table 1.

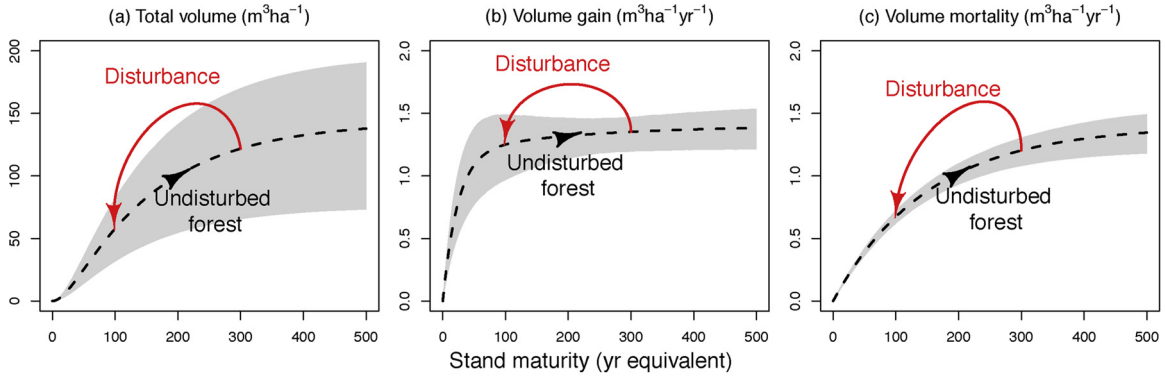

Fig. 2. Total volume and annual volume changes along a forest maturity axis. (a) Total volume; (b) annual volume gain; (c) annual volume mortality. Parameter values are from calibration with Paracou station data: the middle dashed lines are the maximum likelihood prediction, with the arrowheads representing the direction of changes in the absence of disturbances, and the shaded areas are the 95% credibility intervals on predictions. The red arrows represent the sudden decrease in forest maturity caused by a large disturbance. (For interpretation of the references to color in this figure legend, the reader is referred to the web version of this article.)

$$\begin{cases} g(t) = \frac{\alpha_G \times \beta_G}{\theta - \beta_G}(e^{-\beta_G t} - e^{-\theta t}) + \alpha_M \left(1 - \frac{\theta \times e^{-\beta_M t} - \beta_M \times e^{-\theta t}}{\theta - \beta_M}\right) \\ m(t) = \alpha_M \times (1 - e^{-\beta_M t}) \end{cases} \quad (10)$$

The volume potential of the forest stand (*i.e.* the volume at full capacity) is:

$$\text{vmax} = \lim_{t \to \infty}(V(t)) = \frac{\alpha_G - \alpha_M}{\theta} \quad (11)$$

All calculation details (equation solving, limits and constraints on parameters) are in Appendix D.

The effect of logging on commercial species. Only a proportion of the total volume is made of commercial species (*i.e.* species that have a merchantable value): we define $V_k^* = \omega_k \times V(t_k)$ the volume of commercial species at census k, where ω_k is the proportion of commercial species (as a % of total volume) and t_k the maturity. Selective logging targets commercial species. Depending on the logging techniques and the precision of timber harvesting, logging can cause a varying amount of damage to the residual stand.

Let δV be the total volume loss caused by logging. Part of this volume loss is the extracted volume (*Vext*), *i.e.* the volume of commercial trees that have been purposely felled; the rest is the incidental damage to non-commercial trees. The extracted volume is modelled as:

$$\text{Vext} = \omega_0^{1-\psi} \times \delta V \quad (12)$$

where ω_0 is the initial proportion of commercial species (prior to logging), $\psi \leq 1$ is the precision of tree harvesting (*i.e.* how well it targets commercial species): if $\psi = 1$, $\delta V = Vext$: all the volume loss is intentional and there is no incidental damage. If $\psi = 0$, $Vext = \omega_0 \times \delta V$: the volume loss caused by logging (harvested trees + incidental damage) is not directional and affects randomly commercial and non commercial trees, in the same proportion as their occurrence in the forest. If $\psi < 0$, $Vext < \omega_0 \times \delta V$: logging affects particularly non-commercial species, which can be the specific case of silvicultural treatments when the largest non-commercial trees are purposely killed to release competition.

Logging thus changes the proportion of commercial species: let ω_0 be the initial proportion of commercial species and ω_1 the post-logging proportion of commercial species. We have:

$$\omega_1 = \frac{V_0^* - \text{Vext}}{V_0 - \delta V} = \omega_0 \times \frac{1 - \omega_0^{-\psi} \times \frac{\delta V}{V_0}}{1 - \frac{\delta V}{V_0}} \quad (13)$$

with V_0^* the initial commercial volume, V_0 the initial total volume, δV the total volume loss caused by logging, *Vext* the extracted commercial volume and $\psi \leq 1$ the logging precision.

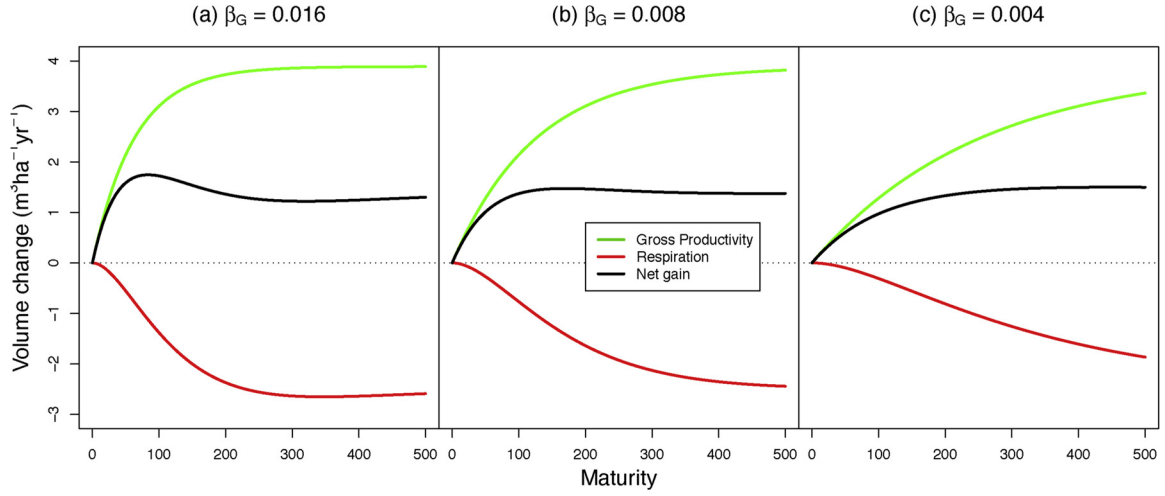

Fig. 3. Illustrative example of the hump-shaped net volume gain (black) when defined as the difference of gross volume productivity (green) and respiration (red). Parameters have been set to their maximum likelihood value in Paracou, except for the gross productivity rate β_G that decreases from (a) 0.016, (b) 0.008 to (c) 0.004 (the maximum likelihood value in Paracou is $\beta_G = 0.0063$). The hump can be more or less pronounced depending on parameter values, giving some flexibility to the relationship between the forest maturity and the net volume gain. (For interpretation of the references to color in this figure legend, the reader is referred to the web version of this article.)

Modelling recruitment. In the absence of further information, we make the conservative assumption that the growth and mortality of trees > 50 cm DBH do not differ between commercial and none commercial species. However, if the proportion of commercial volume ω differs between trees ≥50 cm DBH and trees < 50 cm DBH (as can happen when big commercial trees are selectively logged, decreasing the proportion of commercial volume in trees ≥50 cm DBH), the proportion of commercial volume can recover through the recruitment of trees from DBH < 50 cm to DBH > 50 cm. Let pR_j be the proportion of volume gain from the recruitment of trees < 50 cm DBH to ≥50 cm DBH (the remaining volume gain comes from the growth of trees already DBH ≥50 cm DBH) j years after logging. The proportion of commercial volume in recruited trees is not significantly different from the pre-logging proportion of commercial volume ω_0 (see Appendix A, Fig. A2). We thus have:

$$V(t_{j+1}) \times \omega_{j+1} = V(t_j) \times \omega_j + g(t_j)(\underbrace{\omega_0 \times \mathrm{pR}_j}_{\text{recruitment}} + \underbrace{\omega_j \times (1 - \mathrm{pR}_j)}_{\text{growth}}) - m(t_j) \times \omega_j \quad (14)$$

with pR_j the proportion of recruitment (over the total volume gain $g(t_j)$) j years after logging, and t_j the maturity of the plot j years after logging. We model the proportion of recruitment of trees < 50 cm DBH as a function of the total volume $V(t_j)$:

$$\mathrm{logit}(\mathrm{pR}_j) = \gamma_0 + \gamma_1 \times \ln(V(t_j)) \quad (15)$$

In this model, the proportion of recruitment is 1 when the total volume is null and decreases thereafter. Observations and predictions in Paracou are presented in Appendix A, Fig. A3.

2.4. Inference

Bayesian hierarchical models were inferred through MCMC methods using an adaptive form of the Hamiltonian Monte Carlo sampling (Carpenter et al., 2015). Codes were developed using the R language (R Development Core Team, 2008). We hereafter explicit the models that were inferred. Parameters priors distribution are reported in Table E1.

Covariance structure. In this study we have data from 12 plots, all from a single area of about 500 ha. We assume that all plots have similar disturbance history prior to logging and that they consequently have the same initial forest maturity t_0. For control plots p, we thus have $t_{p,a} = t_0$, with $t_{p,1}$ the maturity at first census. For disturbed plots, the forest maturity at the first census after the disturbance (1987 for logged plots without timber stand improvement, and 1990 for plots with timber stand improvement) is $t_{p,1} = t_0 - tloss_p$ where $tloss_p$ is the maturity loss caused by disturbance in plot p. To account for inter-plot variation, we add a random effect on $vmax_p$ assuming that plots have different productivity potentials:

$$\mathrm{vmax}_p \sim \mathcal{N}(\mu_{\mathrm{vmax}}, \sigma^2_{\mathrm{vmax}}) \quad (16)$$

where μ_{vmax} and σ_{vmax} are the hyperparameters (respectively the mean and standard deviation) of the distribution of $vmax_p$. All other parameters (α_M, β_G, β_M, θ) do not vary between plots. Parameter $\alpha_{G,p}$ for plot p is mathematically deduced from other parameter values:

$$\alpha_{G,p} = \theta \times \mathrm{vmax}_p + \alpha_M \quad (17)$$

Total volume. The total volume of plot p at census k was modelled as:

$$V_{p,k} \sim \ln \mathcal{N}(\mu v_{p,k}, \sigma^2_V) \quad (18)$$

with σ_V the volume's standard deviation and $\mu v_{p,k}$ the mean, which value was deduced from Eqs. (9) and (17):

$$\begin{aligned}\mu v_{p,k} =& \frac{\alpha_{G,p} - \alpha_M}{\theta} - \frac{\alpha_{G,p}}{\theta} \times \frac{\theta \times e^{-\beta_G t_{p,k}} - \beta_G \times e^{-\theta t_{p,k}}}{\theta - \beta_G} + \frac{\alpha_M}{\theta} \times \frac{\theta \times e^{-\beta_M t_{p,k}} - \beta_M \times e^{-\theta t_{p,k}}}{\theta - \beta_M} \\ \mu v_{p,k} =& \mathrm{vmax}_p - \left(\mathrm{vmax}_p + \frac{\alpha_M}{\theta}\right) \times \frac{\theta \times e^{-\beta_G t_{p,k}} - \beta_G \times e^{-\theta t_{p,k}}}{\theta - \beta_G} + \frac{\alpha_M}{\theta} \times \frac{\theta \times e^{-\beta_M t_{p,k}} - \beta_M \times e^{-\theta t_{p,k}}}{\theta - \beta_M}\end{aligned} \quad (19)$$

Disturbance intensity and extracted volume. The volume loss caused by disturbance δV (in $\mathrm{m^3\,ha^{-1}}$), analogous to a disturbance intensity, is the difference (in each disturbed plot) between the pre-disturbance volume (in 1986 in Paracou) and the volume at the first post-disturbance census. For selectively-logged plots, the first post-disturbance census is 1987; in plots that underwent silvicultural treatments, over-mortality from tree poisoning and girdling lasted for as long as 4 years, the first post-disturbance census was then set to 1990. The extracted volume *Vext* is the volume of harvested trees (in $\mathrm{m^3\,ha^{-1}}$).

All plots p in Paracou were subdivided in 4 subplots j, and for each subplot the logging efficiency $\omega\mathrm{ext}_{p,j} = \frac{\mathrm{Vext}_{p,j}}{\delta V_{p,j}}$ and the proportion of commercial volume $\omega_{0,p,j}$ were assessed. We then modelled the logging efficiency as:

$$\omega\mathrm{ext}_{p,j} \sim \mathscr{B}\mathrm{eta}(\alpha_{p,j}, \beta_{p,j}) \quad (20)$$

where $\alpha_{p,j} > 0$ and $\beta_{p,j} > 0$ are the shape parameters of the beta distribution. According to Eq. (12), we modelled the mean of the distribution as:

$$E(\omega\mathrm{ext}) = \omega_{0,p,j}^{(1-\psi_T)} = \frac{\alpha_{p,j}}{\alpha_{p,j} + \beta_{p,j}} \quad (21)$$

with ψ_T the precision of logging, defined in the conceptual framework, and T the logging treatment, either conventional logging or timber stand improvement. To have a variance that is null when $\omega_0 = 0$ and $\omega_0 = 1$ (where ωext is known with certainty, being resp. 0 and 1) and satisfy the conditions $\alpha_{p,j} > 0$ and $\beta_{p,j} > 0$, we modelled the variance of the beta distribution as:

$$\mathrm{Var}(\omega\mathrm{ext}) = E(\omega\mathrm{ext})^2 \times (1 - E(\omega\mathrm{ext})) \times \epsilon_T \quad (22)$$

with $\epsilon_T > 0$ an error parameter. The data and results are presented in Appendix A.

Cumulative volume changes. To avoid focusing on yearly fluctuations and improve our predictive strength, instead of annual volume changes we used, to infer the VDDE model, cumulative volume changes, *i.e.* the annual volume changes integrated over time (as suggested for example in Walters, 1999; Thompson et al., 2001). Cumulative volume growth (cVg) and mortality (cVm) are defined as:

$$\begin{cases} \mathrm{cVg}_{p,1} = \mathrm{cVm}_{p,1} = 0 \\ \forall\, k \geq 2, \begin{cases} \mathrm{cVg}_{p,k} = \sum_{j=2}^{k} \Delta\mathrm{Vg}_{p,j} \times (t_j - t_{j-1}) \\ \mathrm{cVm}_{p,k} = \sum_{j=2}^{k} \Delta\mathrm{Vm}_{p,j} \times (t_j - t_{j-1}) \end{cases} \end{cases} \quad (23)$$

with p the plot and k the census. We model cumulative volume changes as follows:

$$\begin{cases} \mathrm{cVg}_{p,k} \sim \ln \mathcal{N}(\mu g_{p,k}, \sigma^2_G) \\ \mathrm{cVm}_{p,k} \sim \ln \mathcal{N}(\mu m_k, \sigma^2_M) \end{cases} \quad (24)$$

with σ_G and σ_M the standard deviations and $\mu g_{p,k}$ and $\mu m_{p,k}$ the means at census k and in plot p of cumulative volume gain and mortality resp.:

Table 1
Parameters posterior descriptions. We give the median value, 95% credibility interval (CI) and the maximum likelihood value of the VDDE model parameters: t_0 initial forest maturity; *vmax* maximum volume potential, α_M maximum volume mortality; β_G convergence rate of volume growth, β_M convergence rate of volume mortality, θ relative metabolic volume loss, σ_V, σ_G, σ_M standard deviation of volume, cumulative volume gain and cumulative volume mortality resp.

Parameter	Name	95% CI	Max. likelihood value
t_0	Initial forest maturity	186–238	212
vmax	Maximum volume potential	109–261	126
α_M	Maximum volume mortality	1.10–1.44	1.22
β_G	Productivity convergence rate	$(7.32–13.8) \times 10^{-3}$	9.97×10^{-3}
β_M	Mortality convergence rate	$(6.93–11.3) \times 10^{-3}$	9.20×10^{-3}
θ	Relative metabolic volume loss	$(6.82–16.54) \times 10^{-3}$	1.04×10^{-2}
γ_0	Intercept of the recruitment model	1.87–2.74	2.29
γ_1	Slope of the recruitment model	(−0.516) – (−0.295)	−0.400
σ_V	Volume standard deviation	0.06–0.017	0.059
σ_G	Cum. volume gain standard deviation	0.196–0.243	0.227
σ_M	Cum. volume mortality standard deviation	0.464–0.521	0.512
σ_R	Proportion of recruitment standard deviation	0.560–0.673	0.611

$$\mu g_{p,k} = \int_{t_{p,1}}^{t_{p,k}} g(t)\mathrm{d}t = \frac{(\mathrm{vmax}_p \times \theta + \alpha_M) \times \beta_G}{\theta - \beta_G}\left(\frac{e^{-\beta_G t_{p,1}} - e^{-\beta_G t_{p,k}}}{\beta_G} - \frac{e^{-\theta t_{p,1}} - e^{-\theta t_{p,k}}}{\theta}\right) + \alpha_M\left((t_{p,k} - t_{p,1}) - \frac{\frac{\theta}{\beta_M} \times (e^{-\beta_M t_{p,1}} - e^{-\beta_M t_{p,k}}) - \frac{\beta_M}{\theta} \times (e^{-\theta t_{p,1}} - e^{-\theta t_{p,k}})}{\theta - \beta_M}\right) \quad (25)$$

and

$$\mu m_{p,k} = \int_{t_{p,1}}^{t_{p,k}} m(t)\mathrm{d}t = \alpha_M\left((t_{p,k} - t_{p,1}) - \frac{e^{-\beta_M t_{p,1}} - e^{-\beta_M t_{p,k}}}{\beta_M}\right) \quad (26)$$

where $t_{p,k}$ the forest maturity of plot p at census k.

Proportion of commercial volume in recruited trees. We infer the relationship between the total volume $V_{p,k}$ in plot p at census k and the proportion of commercial volume in recruited trees $pR_{p,k}$ according to Eq. (15):

$$\mathrm{logit}(\mathrm{pR}_{p,k}) \sim \mathcal{N}(\gamma_0 + \gamma_1 \times \ln(V_{p,k}),\ \sigma_R^2) \quad (27)$$

where γ_0 and $\gamma_1 > 0$ are resp. the intercept and slope of the relationship, and σ_R the standard deviation.

Validation. To evaluate the predictiveness of the VDDE model we use the first 15 years post-logging (approximately half of the censused period) to calibrate the model, and make predictions over the validation period (≥16 years post-logging). Predictions are then compared with the original data (Fig. 5).

2.5. Simulations

To illustrate some possible uses of the VDDE model, we simulated commercial volume recovery at our site under (i) current conditions and (ii) scenarios reflecting possible effects of future climate changes on disturbance regimes.

Current conditions. Commercial volume recovery at the end of a cutting cycle in Paracou conditions, depending on the logging intensity (extracted volume in $\mathrm{m^3\,ha^{-1}}$), on the cutting cycle length and on the initial proportion of commercial timber was assessed with the following steps: (a) a set of parameters is randomly picked from the parameter posterior distribution; (b) for every values of logging intensity *Vext* between 0 and $30\,\mathrm{m^3\,ha^{-1}}$, we calculate the volume loss $\delta V = \mathrm{Vext} \times \omega_0^{\psi-1}$ and the corresponding post-logging maturity t_1 estimated as: $V(t_1) = V(t_0) - \delta V$, with $V(t_0)$ the volume at the initial maturity t_0 and $V(t_1)$ the volume at the post-logging maturity, given the set of parameters from (a); (c) the post-logging proportion of commercial timber ω_1 is calculated with Eq. (13), with the initial proportion of commercial timber ω_0 being either 10%, 20%, 50% or 100% (in the latter case, $\omega_1 = \omega_0 = 1$), and the proportion ωf of commercial volume at the end of the cutting cycle is estimated with Eq. (14). (d) the commercial volume recovery is then estimated as:

$$\mathrm{Vrec} = V(t_1 + \mathrm{trot}) \times \omega_f - V(t_1) \times \omega_1 \quad (28)$$

with *trot* the cutting cycle length, between 5 and 100 yr. (e) steps (a–d) are repeated with 1000 sets of parameters and summary statistics are then calculated.

In the context of global changes. To illustrate the potential effect of anthropogenic impacts on future volume stocks, we tested how sensitive our results were to modifications in mortality (parameter α_M) and initial maturity (parameter t_0). The total volume was simulated under the hypothesis of a decrease in initial maturity (caused for example by increased frequency of disturbances), and an increase of volume mortality, following the steps: (a) a set of parameters is randomly picked from the posterior distribution; (b) new parameters are calculated: $\alpha'_M = (1 + \pi_M) \times \alpha_M$ (π_M between 0 and 1, corresponding to an increase in mortality between 0% and 100%) and $t'_0 = (1 - \pi_t) \times t_0$ (π_t between 0 and 1, corresponding to a decrease in initial maturity between 0 and 100%); (c) total volume predictions are made with those new sets of parameters; (d) steps (a–c) are repeated with 1000 sets of parameters and summary statistics are calculated.

3. Results and discussion

3.1. Accuracy of the model predictions

In this study, we developed an original model that combines stocks (here total volumes) and fluxes (here volume changes) estimation in one single integrative framework. Stocks are the integrated resultant of fluxes, and the estimation of one flux affects the estimation of the others. Parameters posterior, calibrated with Paracou data, are reported in Table 1. The goodness of prediction of the volume recovery is illustrated in Figs. 4 and B.4. With this rather simple model, we were able to predict the variability of trajectories in total volume recovery for the Paracou dataset (Fig. 4). When calibrating the VDDE model with only the first 15 years of post-logging data (i.e. approx. half of the censused

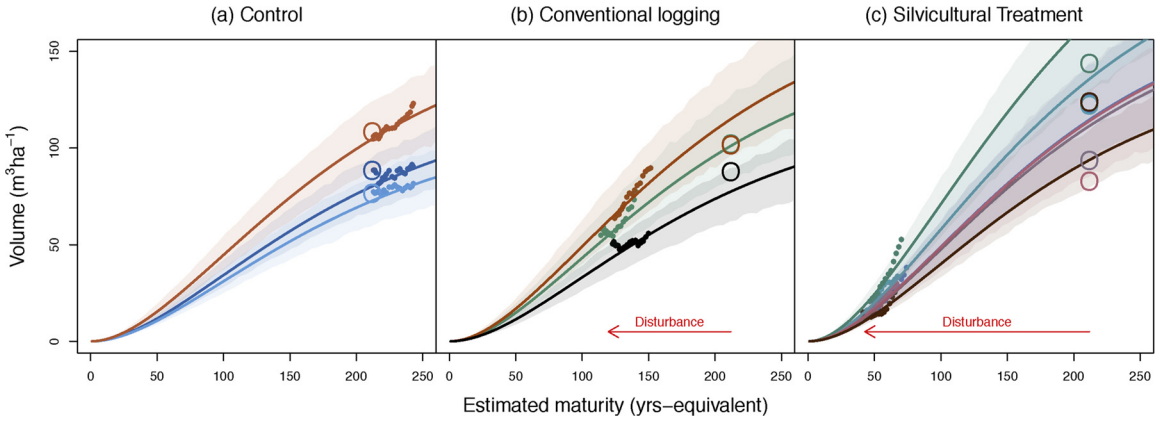

Fig. 4. Predicted and observed trajectories of total volumes in Paracou plots. (a) In control plots. (b) In moderately-disturbed plots (selective logging). (c) In intensively-disturbed plots (selective logging, fuelwood logging, poison girdling). Each plot is represented by a colour. Points represent observed total volumes (*y*-axis) plotted against their predicted maturity (*x*-axis, max-likelihood value), with the large empty dots being the initial total volume (before disturbance for disturbed plots). Lines are the predicted trajectories (max-likelihood value) with the shaded areas being the corresponding 95% credibility intervals. In panels (b) and (c), the arrow represents the effect of logging and additional treatments on the estimated forest maturity. (For interpretation of the references to color in this figure legend, the reader is referred to the web version of this article.)

period), predictions on the last 10–15 years of data (Fig. 5) were still satisfyingly accurate. The predicted pre-logging maturity value is 212 [186–238] yrs-equivalent (Table 1); this does not mean that the forest has 212 years but rather that it would take an estimated 212 years for the forest to reach its pre-logging state in the absence of disturbance. Logging provokes an estimated loss of maturity 90 [62-117] yrs-equivalent, and an additional 72 [64–80] yrs-equivalent after silvicultural treatments (Fig. 4).

3.2. Calibration data may come from diverse sources

One of the main advantages of the VDDE modelling framework is the basic requirement in terms of calibration data. Only measurements of trees above 50 cm are needed, which are rather easy to measure (typically 35 trees ≥50 cm DBH per ha in the tropics (Alder and Synnott, 1992), and 22 to 32 trees per ha in Paracou) and can thus be measured on wide areas covered by National Forest Inventories.

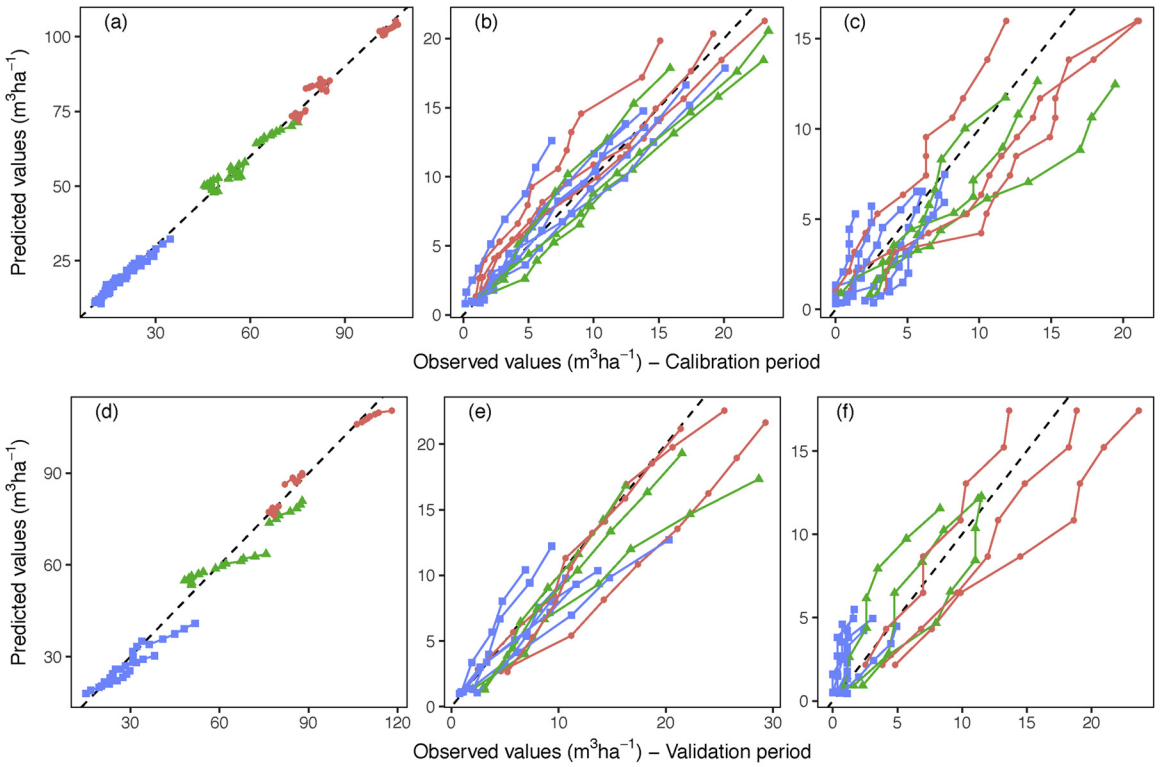

Fig. 5. Predictions vs. observations from the calibration and validation periods in Paracou. All upper panels (a–c) represent data from the calibration period (first 15 years of post-logging observations) and all lower panels (d–f) represent the data from the validation period (more than 15 years after logging); *x*-axes are observations and *y*-axes are maximum-likelihood predictions. Red dots are control plots, green triangles are logged plots, and blue squares are logged plots with silvicultural treatments (poison girdling and fuelwood harvest). (a, d) Total volume ($m^3\,ha^{-1}$). (b, e) Cumulative volume gain. (c, f) Cumulative volume mortality. (For interpretation of the references to color in this figure legend, the reader is referred to the web version of this article.)

Therefore, the VDDE model could be calibrated on a wide range of readily available data. The only restriction lies in the fact that the VDDE model requires at least 2 censuses to estimate total volume stocks and changes. Fortunately, many territories are currently implementing long-term monitoring of their forests under the REDD+ scheme (Maniatis and Mollicone, 2010) and these datasets could be fruitfully used to calibrate the VDDE model. Similarly, in the Brazilian Amazon, logging concessions in national forests are required to have Permanent Sample Plots (1 ha for every 250 ha of logged forests) (Balieiro et al., 2010) that could also be used to estimate the potential for volume recovery at concession level, or wider scale when aggregated. Static data can also be used to calibrate the VDDE model, by adding the measurements of total volume stocks to the overall likelihood of the model. This means that data such as static national inventories can also greatly help improve estimates of total volume and volume recovery. For example, the National Forest Inventory that is being carried out in Brazil aims at measuring all trees above 40 cm DBH in 4 0.2 ha plots in each 20 km × 20 km cell in the whole Brazilian Amazon (Brando et al., 2014). In National forest concessions, the Brazilian Forest Service carries out large inventories of all trees above 50 cm DBH to assess the available timber resource previous to logging (Balieiro et al., 2010).

We developed the VDDE modelling framework to estimate the total volume and commercial volume recovery after selective logging, but this framework could be extended to carbon stocks. Because it is generic enough in terms of ecosystem dynamics, this model could also be used to explore tropical forests resilience to other disturbance types, such as fire and/or drought (Holdsworth and Uhl, 1997; Brando et al., 2014), or even the forest recovery after clear-cutting (Poorter et al., 2016). Results could then be compared to explore the resilience of tropical forests to human and natural disturbances. The methodology may need some adaptations, as some specific problems may require a more complex model.

3.3. Model limitations

While the VDDE model relies upon sensible assumptions, their consequences on the model behaviour may be questioned. For instance, we assumed that the volume change of commercial species is similar to the total volume change during the recovery period. However, because the designation of timber species is generally based on their mechanical wood properties, the commercial species pool may be biased towards hard-wood species (Chave et al., 2009) with generally slow growth rates (Fargeon et al., 2016). However, not all commercial species do grow slowly, as shown by some fast-growing light-wood species (like Balsa (*Ochroma pyramidale*) (Condit et al., 1993)), with interesting mechanical properties (Bossu et al., 2016). The conservative hypothesis of equal relative volume changes is, to our point of view, sensible. It is however worth mentioning that harvesting only very slow growing species would have the effect of lowering the volume recovery, and thus the sustainable logging intensity.

Logging has been proven to lower the height (and thus the volume) of the stand (Rutishauser et al., 2016) resulting in a possible overestimation of timber volume recovery with current allometric equations calibrated in old-growth forests (Guitet et al., 2016). When data becomes available, some new volumetric equations should be calibrated in 2nd harvest forests to update volume estimates.

Assigning the same initial maturity value to all plots may also be questioned: indeed, tropical forests are shaped by very local treefall gap dynamics (Swaine et al., 1987), that could explain small inter-plot variations in forest maturity. From a practical standpoint however, it is difficult to disentangle the inter-plot variations in initial forest maturity from the inter-plot variations in potential volume (*vmax*) with limited time series. In the absence of further information, we thus made the hypothesis that local disturbances from treefall gaps were evened out across our relatively large-size plots (6.25 ha), and that all plots had the same disturbance history.

The model as presented here has been shown to be a useful predictor of post-logging volume recovery at a local scale. However one key challenge for forest management today, especially in the tropics where data is scarce, is to have an understanding of ecological processes at a wider scale, from the landscape to the regional scale (Makela et al., 2000). As stated before, one advantage of the VDDE modelling framework is to allow a variety of widely available calibration data, which makes robust regional estimates of volume recovery possible. To upscale predictions, a possible way is to add spatially-explicit covariates to the model parameters (for instance global maps of climatic (Fick and Hijmans, 2017) or soil variables (Hengl et al., 2014)) as proxies of model parameters.

3.4. Applying the VDDE model to assess logging sustainability

The commercial volume recovered at the end of the cutting cycle is presented in Fig. 6, depending on the cutting cycle length, logging intensity and proportion of commercial volume. The most influential variable on the volume recovery is the proportion of commercial species (increasing proportion of commercial species in panels from left to right on Fig. 6). Both the logging intensity (y-axis) and the length of the cutting cycle (*x*-axis) increases the volume recovery. When the initial proportion of commercial volume is 10% (left panel), the forest hardly recovers more than 5 $m^3\,ha^{-1}$, even after a cutting cycle of 100 years. On the contrary, if all species are commercial (100% of commercial volume), commercial volume recovery following a logging intensity of 20 $m^3\,ha^{-1}$ can be as high as 23 [19–39] $m^3\,ha^{-1}$ at the end of a 60 years cutting cycle.

To be considered sustainable, selective logging should at least allow the recovery of initial timber volumes at the end of each cutting cycle; otherwise, the depletion of timber stocks could undermine the conservation value of managed forests in the long term as the loss of economical value would make them more prone to conversion to other land uses with lower ecological benefits (Edwards et al., 2014). In French Guiana, 75% of timber production depends solely on 3 species: *Dicorynia guianenesis*, *Qualea rosea* and *Sextonia rubra* (French Guiana NFS statistics, unpublished data). In Paracou, the volume of those 3 species represents 20% of the total volume and is consistent with what can be seen over the Guyafor network, a network of permanent plots distributed over the French Guiana permanent forest estate (Piponiot et al., 2016a; Grau et al., 2017). The official cutting cycle length is 65 yr in French Guiana (which is particularly high for the tropics (Blaser et al., 2011)) and the logging intensity for the past 15 years has been 8–29 $m^3\,ha^{-1}$ (Piponiot et al., 2016a). Under such conditions, the results of our model show that only 0–4.1 $m^3\,ha^{-1}$ of commercial volume are recovered at the end of the cutting cycle (Fig. 6): selective logging cannot thus be considered sustainable under current conditions in French Guiana. Compared to other tropical countries, French Guiana's logging policies are especially strict (*e.g.* cutting cycles longer than the usual 30 years) (Blaser et al., 2011). If commercial timber stocks are far from being recovered in French Guiana, there is little chance that logging can be considered sustainable in other tropical countries. It is however worth mentioning that neighbouring countries like Suriname and Brazil harvest a larger variety of commercial tree species (Reis et al., 2010), which might allow higher commercial volume recovery (see Fig. 6). Nevertheless, most studies show that initial volume stocks

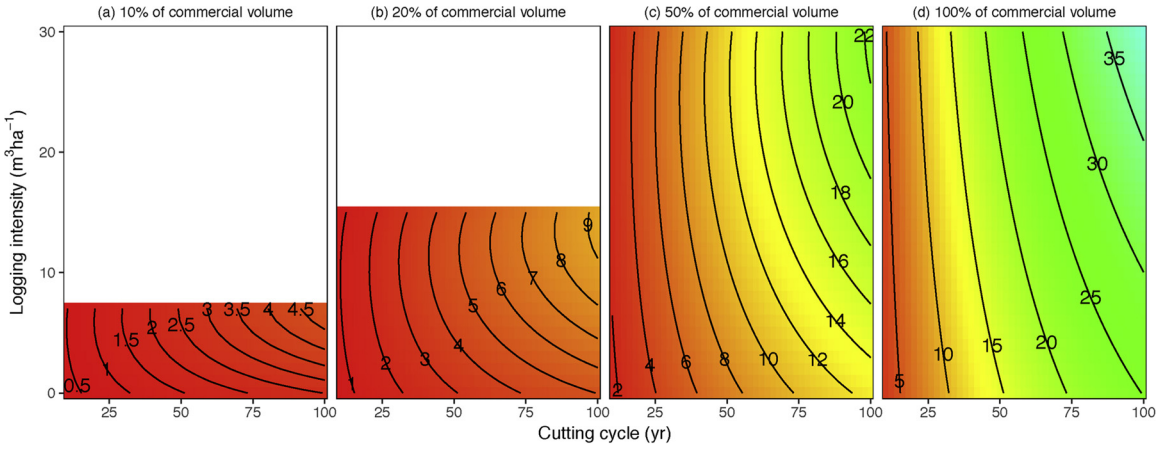

Fig. 6. Commercial volume recovered at the end of the cutting cycle ($m^3\,ha^{-1}$) as a function of cutting cycle length (in years), logging intensity ($m^3\,ha^{-1}$), and initial fraction of commercial species (%), in Paracou conditions. All other parameters are set to their maximum likelihood value. In each panel (a to d), the colors and level lines represent the commercial volume recovered at the end of the cutting cycle. The proportion of commercial species increases from left to right: (a) 10% of total volume is initially composed of commercial species, (b) 20% of total volume is initially composed of commercial species, (c) 50% of total volume is initially composed of commercial species, (d) 100% of total volume is initially composed of commercial species. In all panels, the *x*-axis represents the cutting cycle length; the *y*-axis represents the logging intensity, i.e. the volume of all trees killed during logging operations ($m^3\,ha^{-1}$). The corresponding 95% credibility interval can be found in Fig. C5.

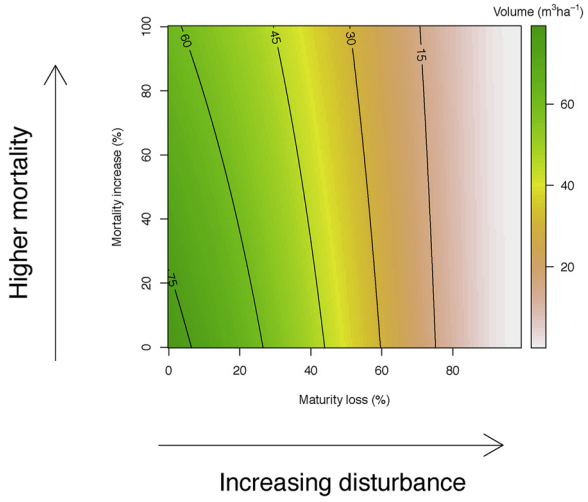

Fig. 7. Total volume ($m^3\,ha^{-1}$) in scenarios with an increase of volume mortality (in % of current mortality in Paracou, *y*-axis) and a decrease of the forest maturity (in % of current mean forest maturity in Paracou, *x*-axis). All other parameters are set to their maximum likelihood value. In each panel, the colors and level lines represent the total volume. The 95% credibility interval (upper and lower bounds) can be found in Fig. C6. (For interpretation of the references to color in this figure legend, the reader is referred to the web version of this article.)

are indeed not recovered in selectively logged forests across the tropics (Putz et al., 2012).

3.5. Applying the VDDE model to assess the effect of diversifying timber sources

For a proportion of commercial species of 100% (*i.e.* the total volume is commercial), the volume recovered at the end of the rotation cycle increases with the logging intensity (Fig. 6). Nevertheless, when the proportion of commercial volume decreases (panel b), increasing the logging intensity can decrease the commercial volume recovery. This is because when logging focuses on only a few commercial species, their proportion at the next logging cycle is inevitably lower (see 2.3) as compared to the other species. This means that even when the total volume is recovered at the end of the cutting cycle, the relative proportion of commercial species will be lower and thus at the next logging cycle the volume recovery will decrease. After a few logging cycles, the proportion of commercial species might be so low that their exploitation may become not economically sound. The smaller the initial pool of commercial species the stronger the depletion. This clearly highlights the benefits of diversifying the pool of harvested species not only at one cutting cycle, but also for changing this pool in time, so that different species are harvested across different cutting cycles. Indeed, the commercial volume recovery is low in the case of a restrictive pool of commercial species (*e.g.* less than $6\,m^3\,ha^{-1}$ after 65 yr in Paracou if only 20% of the total volume is commercial). At the 2nd harvest the available commercial volume will be too low, such that harvesting the same forest stands several times will inevitably mean changing the pool of harvested species at the 2nd harvest.

3.6. Applying the VDDE model to assess timber availability in human-modified forests under climate change

Tropical forests are not spared from ongoing global changes (Malhi et al., 2014): most tropical forests undergo increasing disturbance regimes such as fires, logging, or drought (Lewis et al., 2015). Today, the so-called intact forest landscape in the tropics has been reduced to 20% of the tropical forest area (Potapov et al., 2017), and this proportion is likely to continue decreasing. Future climate is predicted to be hotter and seasonally drier in most tropical landscapes (Stocker, 2014), provoking a decrease in biomass through the increase of tree mortality (Allen et al., 2010). In Amazonian forests, this continuous increase in tree mortality has already been described (Brienen et al., 2015). Within our modeling framework, an increased disturbance regime will

inevitably decrease the forest maturity (we simulated a 0–100% decrease of forest maturity), and a drier climate will inevitably increase the volume mortality (Fig. 7). For instance, biomass mortality has increased by approximately 30% in Amazonian Permanent sample plots between 1985 and 2010 (Brienen et al., 2015). For a similar increase in volume mortality, total volume stocks in Paracou are predicted to decrease from 80 (68–167) to 65 (86–153) $m^3\,ha^{-1}$, *i.e.* a 19% decrease (numbers between brackets are the 95% credibility interval). And if those forests also suffer from increasing disturbances and their forest maturity subsequently decreases, for example by 40%, then the total volume would be 47 (40–100) $m^3\,ha^{-1}$, *i.e.* a 41% decrease. The combined effect of an increase of mortality and of the disturbance regime could thus seriously lower available timber resource in tropical forests. This has to be taken into account for future scenarios of timber provision in increasingly human-modified forests.

4. Conclusion

In this study we present an original modelling approach of timber volume recovery in tropical forests. As a case study, we assess the volume recovery potential of a selectively logged forest in French Guiana. We show that under current conditions, selective logging is not sustainable insofar as the commercial volume, which is the main productive value of a logged forest, is not recovered at the end of a typical logging cycle. We also predict timber availability in the case of an increase mortality and a decrease of forest maturity, that will likely be triggered by future climate change and human disturbances such as fires, clearcuts and logging. The main advantages of the modelling framework presented here are threefold: (i) it can be calibrated with widely available data (*i.e.* the volume of trees $\geq$50 cm DBH), (ii) it can explicitly integrate the effect of disturbances and (iii) it is generic enough to be applied for instance to carbon stocks. To provide meaningful insights to forest managers and policy makers, this model should now be applied to a larger scale, integrating data from permanent forest plots as well as national forest inventories.

Availability of data and materials

Data and R codes will be made available on an online repository.

Competing interests

The authors declare no competing interest.

Funding

This study was partially funded by the GFclim project (FEDER 20142020, Project GY0006894), an Investissement dAvenir grant of the ANR (CEBA: ANR-10-LABEX-0025) and carried out in the framework of the Tropical managed Forests Observatory (TmFO), supported by the Sentinel Landscape program of CGIAR (Consultative Group on International Agricultural Research) – Forest Tree and Agroforestry Research Program.

Author's contributions

Acquisition of data: BH. Conception & design: CP, BH. Model Development: CP, BH. Data analysis & interpretation: CP, BH. Drafting the manuscript: CP. Manuscript revision: BH, ER, PS, LM, GD, LD, CP.

Acknowledgements

We are in debt with all technicians and colleagues who helped setting up the plots and collecting data over years. Without their precious work, this study would not have been possible and they may be warmly thanked here. We would also like to thank the 2 anonymous reviewers for their in-depth reading and valuable comments.

Appendix A. Proportion of commercial volume

Figs. A1–A3

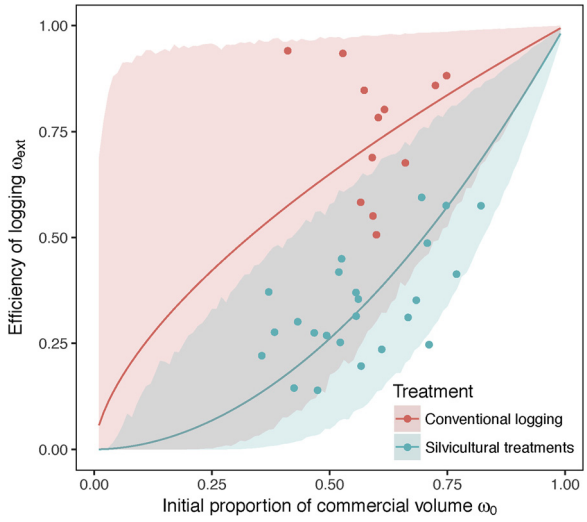

Fig. A1. Efficiency of selective logging ωext as a function of the proportion of commercial species ω_0. The efficiency of logging $\omega\text{ext} = \frac{\text{Vext}}{\delta V}$ was modelled as $\omega ext = {\omega_0}^{1-\psi}$, and the model was calibrated for subplots (4 subplots by plot, 1.5625 ha each) that underwent conventional logging (red dots) and intensive logging with timber stand improvement (green dots). The red and green lines are the maximum likelihood prediction of the model for conventional logging and silvicultural treatments resp., and the shaded areas are the 95% credibility intervals.

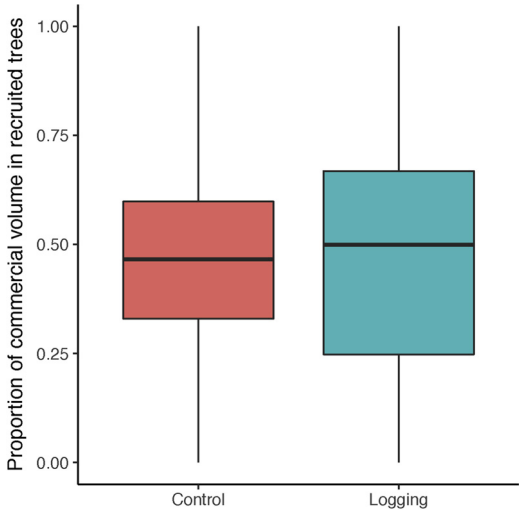

Fig. A2. Comparison of the proportion of commercial volume in recruited trees in control plots and conventionally logged plots in Paracou.

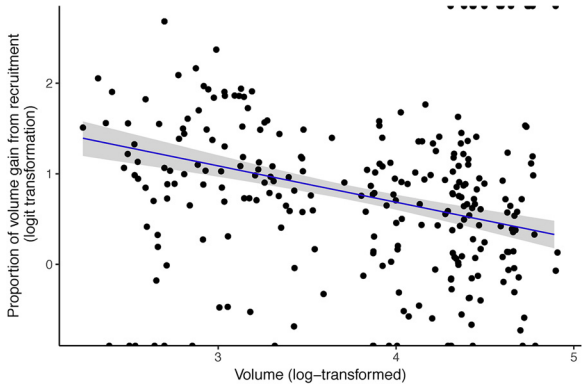

Fig. A3. Proportion of volume gain from recruitment (*pR*, on the *y*-axis, after a logit-transformation) as a function of the total volume (*x*-axis, after log-transformation). Dots are observations in Paracou, the blue line is the linear model prediction, and the shaded area is the associated 95% credibility interval. (For interpretation of the references to color in this figure legend, the reader is referred to the web version of this article.)

Appendix B. Goodness of fit

Fig. B4

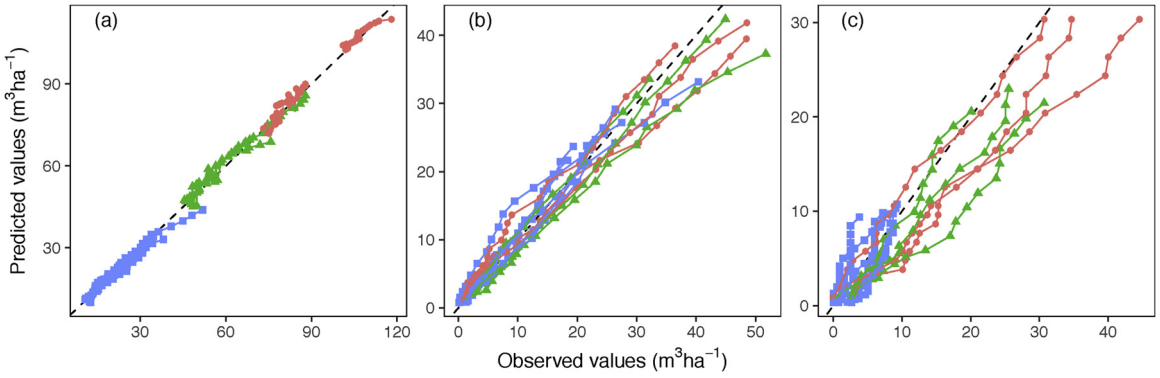

Fig. B4. Goodness of fit of the model predictions to Paracou data. Observed values of (a) total volume, (b) cumulative volume gain, (c) cumulative volume mortality are on the *x*-axis, while the predicted values are on the *y*-axis. Red dots are control plots, green triangles are logged plots and blue squares are logged plots with silvicultural treatments (poison gridling and fuelwood harvest). (For interpretation of the references to color in this figure legend, the reader is referred to the web version of this article.)

Appendix C. 95% credibility intervals of simulation predictions

Figs. C5 and C6

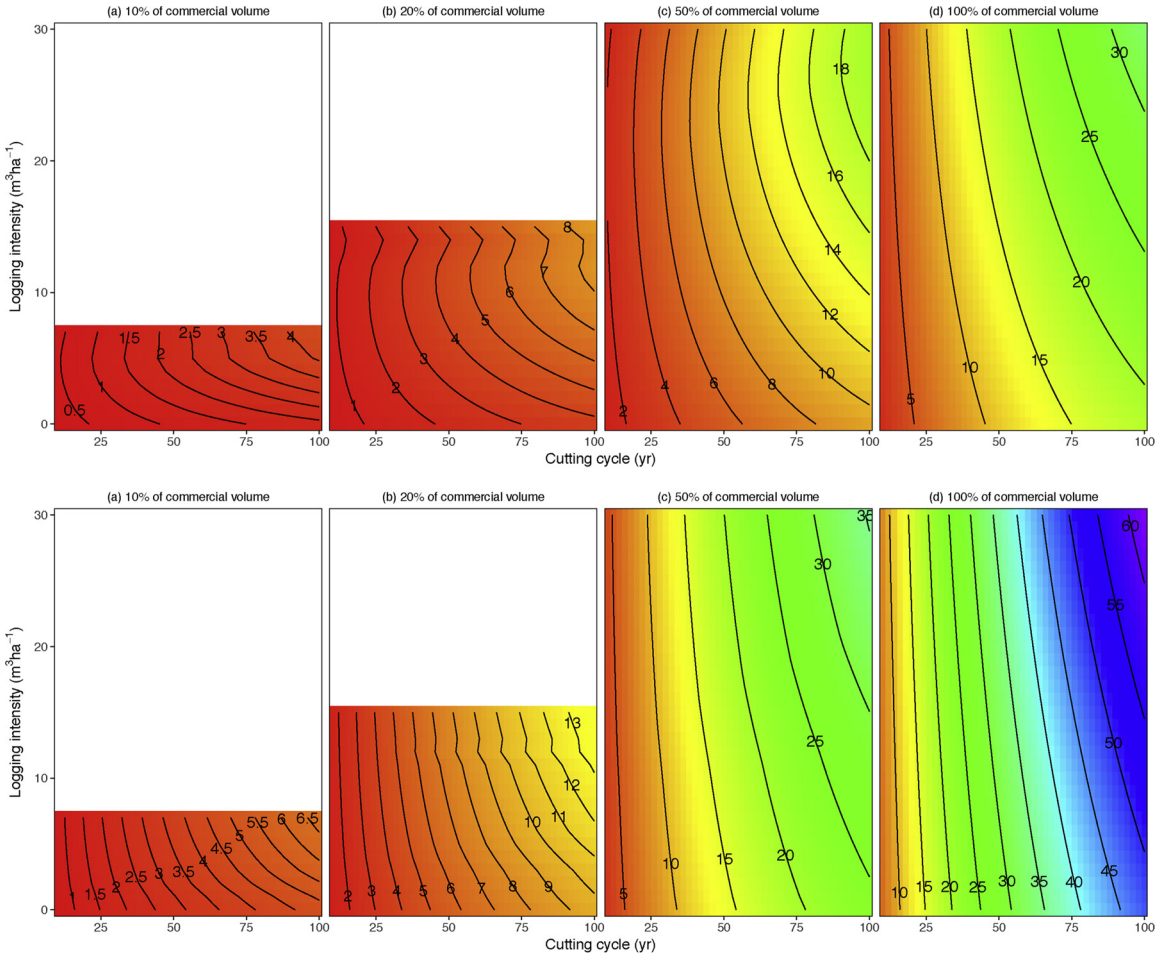

Fig. C5. 95% credibility interval of commercial volume recovered at the end of the cutting cycle ($m^3\,ha^1$) as a function of cutting cycle length (in years), logging intensity ($m^3\,ha^1$), and initial fraction of commercial species (%), in Paracou conditions. All other parameters are set to their maximum likelihood value. (a) Lower bound (2.5th percentile); (b) upper bound (97.5th percentile). In each panel, the colours and level lines represent the commercial volume recovered at the end of the cutting cycle. The proportion of commercial species increases from left to right: it is lowest in extreme-left panels (10% of total volume belongs to commercial species) and highest in extreme-right panels (100% of total volume). In all panels, the *x*-axis represents the cutting cycle length; the *y*-axis represents the logging intensity, i.e. the volume of all trees killed during logging operations ($m^3\,ha^1$). (For interpretation of the references to color in this figure legend, the reader is referred to the web version of this article.)

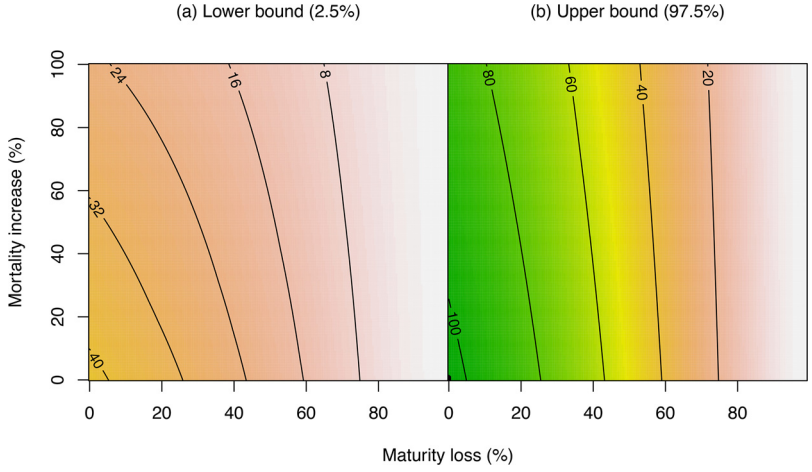

Fig. C6. 95% credibility interval of total volume ($m^3\,ha^1$) in scenarios with an increase of volume mortality (in % of current mortality in Paracou, *y*-axis) and a decrease of the forest maturity (in % of current mean forest maturity in Paracou, *x*-axis). All other parameters are set to their maximum likelihood value. (a) Lower bound (2.5th percentile); (b) upper bound (97.5th percentile). In each panel, the colors and level lines represent the total volume. (For interpretation of the references to color in this figure legend, the reader is referred to the web version of this article.)

Appendix D. Extensive equation material

D.1 Solving the differential equation (8)

According to Eq. (8) we have:

$$\frac{\mathrm{dV}(t)}{\mathrm{dt}} = \alpha_G(1 - e^{-\beta_G t}) - \theta V(t) - \alpha_M(1 - e^{-\beta_M t})$$

Let's solve the nonhomogeneous differential equation of 1st order:

$$\frac{\mathrm{dV}(t)}{\mathrm{dt}} + \theta V(t) = \alpha_G(1 - e^{-\beta_G t}) - \alpha_M(1 - e^{-\beta_M t}) \tag{D.1}$$

We define $u(t) = e^{\theta t}$.
We have:

$$\begin{aligned}(u(t) \times V(t))' &= u'(t) \times V(t) + u(t) \times V'(t)\\ &= \theta e^{\theta t} \times V(t) + e^{\theta t} \times \frac{\mathrm{dV}(t)}{\mathrm{dt}}\\ &= u(t)\left(\frac{\mathrm{dV}(t)}{\mathrm{dt}} + \theta V(t)\right)\\ (u(t) \times V(t))' &= u(t)(\alpha_G(1 - e^{-\beta_G t}) - \alpha_M(1 - e^{-\beta_M t}))\end{aligned} \tag{D.2}$$

Thus:

$$\begin{aligned}u(t) \times V(t) &= \int e^{\theta t}(\alpha_G(1 - e^{-\beta_G t}) - \alpha_M(1 - e^{-\beta_M t}))\mathrm{dt}\\ &= \alpha_G\left(\frac{e^{\theta t}}{\theta} - \frac{e^{(\theta-\beta_G)t}}{\theta-\beta_G}\right) - \alpha_M\left(\frac{e^{\theta t}}{\theta} - \frac{e^{(\theta-\beta_M)t}}{\theta-\beta_M}\right) + K\\ e^{\theta t} \times V(t) &= e^{\theta t}\left(\alpha_G\left(\frac{1}{\theta} - \frac{e^{-\beta_G t}}{\theta-\beta_G}\right) - \alpha_M\left(\frac{1}{\theta} - \frac{e^{-\beta_M t}}{\theta-\beta_M}\right) + K \times e^{-\theta t}\right)\end{aligned} \tag{D.3}$$

with K a constant, and $\beta_G \neq \theta \neq \beta_M$. Because $V(0) = 0$ (see Eq. (8)), we get:

$$\begin{cases} V(t) = \alpha_G\left(\frac{1}{\theta} - \frac{e^{-\beta_G t}}{\theta-\beta_G}\right) - \alpha_M\left(\frac{1}{\theta} - \frac{e^{-\beta_M t}}{\theta-\beta_M}\right) + K \times e^{-\theta t}\\ V(0) = 0 \end{cases} \tag{D.4}$$

And thus:

$$K = \alpha_G\left(\frac{1}{\theta - \beta_G} - \frac{1}{\theta}\right) - \alpha_M\left(\frac{1}{\theta - \beta_M} - \frac{1}{\theta}\right) \tag{D.5}$$

$$V(t) = \frac{\alpha_G}{\theta}\left(1 - \frac{\theta e^{-\beta_G t} - \beta_G e^{-\theta t}}{\theta - \beta_G}\right) - \frac{\alpha_M}{\theta}\left(1 - \frac{\theta e^{-\beta_M t} - \beta_M e^{-\theta t}}{\theta - \beta_M}\right) \tag{D.6}$$

$$\begin{cases} g(t) = \frac{\alpha_G\beta_G}{\theta-\beta_G}(e^{-\beta_G t} - e^{-\theta t}) + \alpha_M\left(1 - \frac{\theta e^{-\beta_M t} - \beta_M e^{-\theta t}}{\theta - \beta_M}\right)\\ m(t) = \alpha_M(1 - e^{-\beta_M t}) \end{cases} \tag{D.7}$$

D.2 Additional constraints on the model parameters

We have the natural constraint: $\forall t \geq 0$, $V(t) \geq 0$. We here develop the few steps that allowed us to translate this inequality into contraints on the model parameters. To do so we studied the function $V(t)$ limits when $t \to +\infty$ and when $t \to 0$.

Because $\theta > 0$, $\alpha_G > 0$ and $\alpha_M > 0$, we have:

$$\lim_{t\to+\infty}(e^{-\beta_G t}) = \lim_{t\to+\infty}(e^{-\beta_M t}) = \lim_{t\to+\infty}(e^{-\theta t}) = 0 \tag{D.8}$$

$$\begin{aligned}\Rightarrow \lim_{t\to\infty} V(t) &= \tfrac{\alpha_G}{\theta}(1 - 0) - \tfrac{\alpha_M}{\theta}(1 - 0)\\ \lim_{t\to\infty} V(t) &= \tfrac{\alpha_G - \alpha_M}{\theta}\end{aligned} \tag{D.9}$$

$$\lim_{t\to\infty} V(t) \geq 0 \Leftrightarrow \alpha_G \geq \alpha_M \tag{D.10}$$

When $t = 0$, there is no volume (by definition): $V(0) = 0$. Consequently, for the volume to take positive values near $t = 0$, we must have $\frac{\mathrm{dV}}{\mathrm{dt}} \geq 0$ near $t = 0$ (i.e. the volume can only increase, else it will take negative values, which is absurd).

$$\begin{aligned}\frac{dV}{dt} &= g(t) - m(t)\\ &= \alpha_G(1 - e^{-\beta_G t}) - \theta V(t) - \alpha_M(1 - e^{-\beta_M t})\\ &= \alpha_G(1 - e^{-\beta_G t}) - \alpha_M(1 - e^{-\beta_M t}) - \alpha_G\left(1 - \frac{\theta e^{-\beta_G t} - \beta_G e^{-\theta t}}{\theta - \beta_G}\right)\\ &+ \alpha_M\left(1 - \frac{\theta e^{-\beta_M t} - \beta_M e^{-\theta t}}{\theta - \beta_M}\right)\\ &= e^{-\beta_G t}\left(\frac{\alpha_G\beta_G}{\theta - \beta_G}\right) - e^{-\beta_M t}\left(\frac{\alpha_M\beta_M}{\theta - \beta_M}\right) - e^{-\theta t}\left(\frac{\alpha_G\beta_G}{\theta - \beta_G} - \frac{\alpha_M\beta_M}{\theta - \beta_M}\right)\end{aligned} \tag{D.11}$$

By using the Taylor series (of order 1) of the exponential function when $t \to 0$, we get:

$$\begin{aligned}\frac{dV}{dt} &\sim -t \times \beta_G\left(\frac{\alpha_G\beta_G}{\theta - \beta_G}\right) + t \times \beta_M\left(\frac{\alpha_M\beta_M}{\theta - \beta_M}\right) + t \times \theta\left(\frac{\alpha_G\beta_G}{\theta - \beta_G} - \frac{\alpha_M\beta_M}{\theta - \beta_M}\right)\\ \frac{dV}{dt} &\sim t \times (\alpha_G\beta_G - \alpha_M\beta_M)\end{aligned} \tag{D.12}$$

To have an increase in volume (and thus $V(t) \geq 0$) when $t \geq 0$ is close to 0, we must have:

$$\alpha_G \times \beta_G \geq \alpha_M \times \beta_M \tag{D.13}$$

Appendix E. Additional tables

Tables E1 and E2

Table E1
Parameters prior distribution.

Parameter	Prior distribution	Justification
t_0	$\mathscr{U}[100, 300]$	Expected maturity in Paracou
vmax	$\mathscr{U}[\max(V), 3\max(V)]$	*vmax* must be bigger than the max. observed volume, and can harldy be more than 3 times as much
α_M	$\mathscr{U}[0.5, 5]$	Range of observed values for biomass mortality in the Guiana Shield (Johnson et al., 2016) divided by 1.5 (2: carbon:biomass ratio × 0.75: mean wood density in Paracou)
β_G	$\mathscr{U}[0.005, 0.05]$	$60 < t_{95} < 600$[a] yr
β_M	$\mathscr{U}[0.001, \beta_G \times \frac{\alpha_G}{\alpha_M}]$	$t_{95} > 3000$[a] yr and slower than growth
θ	$\mathscr{U}[0.005, 0.05]$	Respiration < $max(vmax) \times 0.05 = 17$ $m^3\,ha^{-1}\,yr^{-1}$
ω_0	$\mathscr{N}(0, 0.001)$	Uninformative prior
ω_1	$\mathscr{N}_{]-\infty,0]}(0, 0.001)$[b]	Negative: *pR* decreases when the volume increases
σ_V	$\mathscr{N}_{[0,2]}(0, 1)$	Positive variance
σ_G	$\mathscr{N}_{[0,2]}(0, 1)$	Positive variance
σ_M	$\mathscr{N}_{[0,2]}(0, 1)$	Positive variance
σ_R	$\mathscr{N}_{[0,+\infty[}(0, 1)$	Positive variance

[a] $t_{0.95}$ is the time when the volume change has reached 95% of its asymptotic value.
[b] $\mathscr{N}_{[a,b]}$ is the normal distribution truncated in [a,b].

Table E2
List of commercial species in Paracou.

Local name	Scientific name	Proportion of initial volume (%)	Proportion of logged volume (%)
Gonfolo	*Qualea rosea*	2.71	26.98
Wapa	*Eperua falcata*	7.96	12.74
Grignon franc	*Sextonia rubra*	1.92	12.53
Angélique	*Dicorynia guianensis*	2.31	9.19
Manil	*Moronobea coccinea*	1.00	4.47
Chawari	*Caryocar glabrum*	0.94	3.86
Wakapu	*Vouacapoua americana*	3.07	2.77
Asao	*Albizia pedicellaris*	0.50	2.38
Maho cigare	*Couratari multiflora*	1.01	1.93
Diagidia	*Tachigali melinonii*	0.79	1.78
Saint martin rouge	*Andira coriacea*	0.46	1.76
Balata pomme	*Chrysophyllum sanguinolentum*	1.17	1.64
Maho cochon	*Sterculia pruriens*	0.98	1.57
Goupi	*Goupia glabra*	1.17	1.40
Dodomisinga	*Parkia nitida*	0.65	1.36
Busi kanambuli	*Simaba sp.*	0.32	1.23
Yayamadou marcage	*Virola surinamensis*	0.31	1.13

(*continued on next page*)

Table E2 (*continued*)

Local name	Scientific name	Proportion of initial volume (%)	Proportion of logged volume (%)
Wakapu gitin	*Recordoxylon speciosum*	0.90	1.04
Parcouri	*Platonia insignis*	0.34	0.98
Alimiao	*Pseudopiptadenia suaveolens*	0.12	0.95
Cèdre	*Ocotea argyrophylla*	0.26	0.84
Balata franc	*Manilkara bidentata*	0.37	0.73
Acacia franc	*Enterolobium schomburgkii*	0.28	0.56
Maho coton	*Pachira dolichocalyx*	0.27	0.53
Inkasa	*Vataireopsis surinamensis*	0.05	0.48
Boco	*Bocoa prouacensis*	2.22	0.45
Kwata kaman	*Parkia pendula*	0.08	0.43
Kaiman udu	*Laetia procera*	0.13	0.41
Bois saint jean	*Protium opacum*	0.17	0.38
Encens	*Schefflera decaphylla*	0.98	0.38
Cèdre cannelle	*Licaria cannella*	0.08	0.34
Dokali	*Brosimum utile*	0.13	0.33
Lebi sali	*Trichilia schomburgkii*	0.18	0.30
Coeur dehors	*Diplotropis purpurea*	0.17	0.29
Kumanti udu	*Aspidosperma sp.*	0.22	0.26
Mapa	*Lacmellea aculeata*	0.24	0.25
Wana kwali	*Vochysia tomentosa*	0.06	0.19
Kwali	*Vochysia guianensis*	0.06	0.19
Saint martin jaune	*Hymenolobium flavum*	0.03	0.16
Simarouba	*Simarouba amara*	0.05	0.16
Gaan moni	*Trattinnickia rhoifolia*	0.13	0.15
Lakasi	*Caraipa racemosa*	0.04	0.13
Canari macaque	*Lecythis zabucajo*	0.17	0.13

Appendix F. Supplementary data

Supplementary data associated with this article can be found, in the online version, at https://doi.org/10.1016/j.ecolmodel.2018.05.023.

References

Alder, D., Synnott, T., 1992. Permanent Sample Plot Techniques for Mixed Tropical Forest. Oxford Forestry Institute. http://www.fao.org/sustainable-forest-management/toolbox/tools/tool-detail/en/c/340781/.

Allen, C.D., Macalady, A.K., Chenchouni, H., Bachelet, D., McDowell, N., Vennetier, M., Kitzberger, T., Rigling, A., Breshears, D.D., Hogg, E.T., Gonzalez, P., Fensham, R., Zhang, Z., Castro, J., Demidova, N., Lim, J.-H., Allard, G., Running, S.W., Semerci, A., Cobb, N., 2010. A global overview of drought and heat-induced tree mortality reveals emerging climate change risks for forests. For. Ecol. Manag. 259 (4), 660–684. http://dx.doi.org/10.1016/j.foreco.2009.09.001. arXiv:1011.1669v3.

Asner, G.P., Keller, M., Pereira, R., Zweede, J.C., 2002. Remote sensing of selective logging in Amazonia. Remote Sens. Environ. 80 (3), 483–496. http://dx.doi.org/10.1016/S0034-4257(01)00326-1.

Balieiro, M.R., Espada, A.L.V., Nogueira, O., Palmieri, R., Lentini, M., 2010. As Concessoes de Florestas Públicas na Amazônia Brasileira. http://www.fundovale.org/wp-content/uploads/2016/01/Concessoes-Florestais_ift_imaflora.pdf.

Bawa, K.S., Seidler, R., 1998. Natural forest management and conservation of biodiversity in tropical forests. Conserv. Biol. 12 (1), 46–55. http://dx.doi.org/10.1046/j.1523-1739.1998.96480.x.

Berger, U., Rivera-Monroy, V.H., Doyle, T.W., Dahdouh-Guebas, F., Duke, N.C., Fontalvo-Herazo, M.L., Hildenbrandt, H., Koedam, N., Mehlig, U., Piou, C., Twilley, R.R., 2008. Advances and limitations of individual-based models to analyze and predict dynamics of mangrove forests: a review. Aquat. Bot. 89 (2), 260–274. http://dx.doi.org/10.1016/j.aquabot.2007.12.015. http://linkinghub.elsevier.com/retrieve/pii/S0304377008000090.

Blanc, L., Echard, M., Herault, B., Bonal, D., Marcon, E., Chave, J., Baraloto, C., 2009. Dynamics of aboveground carbon stocks in a selectively logged tropical forest. Ecol. Appl. 19 (6), 1397–1404. http://dx.doi.org/10.1890/08-1572.1.

Blaser, J., Sarre, A., Poore, D., Johnson, S., 2011. Status of Tropical Forest Management 2011, Tech. rep. http://www.itto.int/news_releases/id=2663.

Bossu, J., Beauchêne, J., Estevez, Y., Duplais, C., Clair, B., 2016. New insights on wood dimensional stability influenced by secondary metabolites: the case of a fast-growing tropical species *Bagassa guianensis* Aubl. PLOS ONE 11 (3). http://dx.doi.org/10.1371/journal.pone.0150777.

Brando, P.M., Balch, J.K., Nepstad, D.C., Morton, D.C., Putz, F.E., Coe, M.T., Silverio, D., Macedo, M.N., Davidson, E.A., Nobrega, C.C., Alencar, A., Soares-Filho, B.S., 2014. Abrupt increases in Amazonian tree mortality due to drought-fire interactions. Proc. Natl. Acad. Sci. 111 (17), 6347–6352. http://dx.doi.org/10.1073/pnas.1305499111.

Brienen, R.J.W., Phillips, O.L., Feldpausch, T.R., Gloor, E., Baker, T.R., Lloyd, J., Lopez-Gonzalez, G., Monteagudo-Mendoza, A., Malhi, Y., Lewis, S.L., Vásquez Martinez, R., Alexiades, M., Álvarez Dávila, E., Alvarez-Loayza, P., Andrade, A., Arag ao, L.E.O.C., Araujo-Murakami, A., Arets, E.J.M.M., Arroyo, L., Aymard, G.A., Bánki, C.O.S., Baraloto, C., Barroso, J., Bonal, D., Boot, R.G.A., Camargo, J.L.C., Castilho, C.V., Chama, V., Chao, K.J., Chave, J., Comiskey, J.A., Cornejo Valverde, F., da Costa, L., de Oliveira, E.A., Di Fiore, A., Erwin, T.L., Fauset, S., Forsthofer, M., Galbraith, D.R., Grahame, E.S., Groot, N., Hérault, B., Higuchi, N., Honorio Coronado, E.N., Keeling, H., Killeen, T.J., Laurance, W.F., Laurance, S., Licona, J., Magnussen, W.E., Marimon, B.S., Marimon-Junior, B.H., Mendoza, C., Neill, D.A., Nogueira, E.M., Nú nez, P., Pallqui Camacho, N.C., Parada, A., Pardo-Molina, G., Peacock, J., Pe na-Claros, M., Pickavance, G.C.N., 2015. Long-term decline of the Amazon carbon sink. Nature 519 (7543), 344–348. http://dx.doi.org/10.1038/nature14283. http://www.scopus.com/inward/record.url?eid=2-s2.0-84925302004&partnerID=tZOtx3y1, http://www.scopus.com/inward/record.url?eid=2-s2.0-84925302004%7B&%7DpartnerID=tZOtx3y1.

Burivalova, Z., Sekercioglu, Ç.H., Koh, L.P., 2014. Thresholds of logging intensity to maintain tropical forest biodiversity. Curr. Biol. 24 (16), 1893–1898. http://dx.doi.org/10.1016/j.cub.2014.06.065. http://linkinghub.elsevier.com/retrieve/pii/S0960982214007829.

Cannon, C.H., Peart, D.R., Leighton, M., Kartawinata, K., Leighton, M., Peart David, R., 1994. The structure of lowland rainforest after selective logging in West Kalimantan, Indonesia. For. Ecol. Manag. 67 (1–3), 49–68. http://dx.doi.org/10.1016/0378-1127(94)90007-8. http://www.sciencedirect.com/science/article/pii/0378112794900078%5Cnhttp://ac.els-cdn.com/0378112794900078/1-s2.0-0378112794900078-main.pdf?_tid=5f25b186-940b-11e3-81e7-00000aacb35f&acdnat=1392226411%_924eea2edad54c40bba98edf7f52d5b1.

Carpenter, B., Gelman, A., Hoffman, M.D., Lee, D., Goodrich, B., Betancourt, M., Brubaker, M., Guo, J., Li, P., Riddell, A., 2015. Stan: a probabilistic programming language. J. Stat. Softw. 76 (1). http://dx.doi.org/10.18637/jss.v076.i01. http://www.jstatsoft.org/v76/i01/.

Chambers, J.Q.J., Negron-Juarez, R.I.R., Marra, D.M.D.D.M., Di Vittorio, A., Tews, J., Roberts, D., Ribeiro, G.H.P.M.G., Trumbore, S.E.S., Higuchi, N., 2013. The steady-state mosaic of disturbance and succession across an old-growth Central Amazon forest landscape. Proc. Natl. Acad. Sci. U. S. A. 110 (10), 3949–3954. http://dx.doi.org/10.1073/pnas.1202894110. http://www.pubmedcentral.nih.gov/articlerender.fcgi?artid=3593828&tool=pmcentrez&rendertype=abstract.

Chave, J., Coomes, D., Jansen, S., Lewis, S.L., Swenson, N.G., Zanne, A.E., 2009. Towards a worldwide wood economics spectrum. Ecol. Lett. 12 (4), 351–366. http://dx.doi.org/10.1111/j.1461-0248.2009.01285.x.

Chen, W., Chen, J.M., Price, D.T., Cihlar, J., 2002. Effects of stand age on net primary productivity of boreal black spruce forests in Ontario, Canada. Can. J. For. Res. 32 (5), 833–842. http://dx.doi.org/10.1139/x01-165.

Condit, R., Hubbell, S.P., Foster, R.B., 1993. Identifying fast-growing native trees from the neotropics using data from a large, permanent census plot. For. Ecol. Manage. 62

(1–4), 123–143. http://dx.doi.org/10.1016/0378-1127(93)90046-Pc.
de Avila, A.L., Ruschel, A.R., de Carvalho, J.O.P., Mazzei, L., Silva, J.N.M., Lopes, J.D.C., Araujo, M.M., Dormann, C.F., Bauhus, J., 2015. Medium-term dynamics of tree species composition in response to silvicultural intervention intensities in a tropical rain forest. Biol. Conserv. 191, 577–586. http://dx.doi.org/10.1016/j.biocon.2015.08.004.
R Development Core Team, 2008. Computational Many-Particle Physics. R Foundation for Statistical Computing 739, pp. 409. http://dx.doi.org/10.1007/978-3-540-74686-7. http://www.r-project.org/%5Cnhttp://www.r-project.org.
Edwards, D.P., Tobias, J.A., Sheil, D., Meijaard, E., Laurance, W.F., 2014. Maintaining ecosystem function and services in logged tropical forests. Trends Ecol. Evol. 29 (9), 511–520. http://dx.doi.org/10.1016/j.tree.2014.07.003.
Espírito-Santo, F.D., Gloor, M., Keller, M., Malhi, Y., Saatchi, S., Nelson, B., Junior, R.C.O., Pereira, C., Lloyd, J., Frolking, S., Palace, M., Shimabukuro, Y.E., Duarte, V., Mendoza, A.M., López-González, G., Baker, T.R., Feldpausch, T.R., Brienen, R.J., Asner, G.P., Boyd, D.S., Phillips, O.L., 2014. Size and frequency of natural forest disturbances and the Amazon forest carbon balance. Nat. Commun. 5, 3434. http://dx.doi.org/10.1038/ncomms4434. http://www.ncbi.nlm.nih.gov/pubmed/24643258.
Fargeon, H., Aubry-Kientz, M., Brunaux, O., Descroix, L., Gaspard, R., Guitet, S., Rossi, V., Hérault, B., 2016. Vulnerability of commercial tree species to water stress in logged forests of the Guiana shield. Forests 7 (12), 105. http://dx.doi.org/10.3390/f7050105. http://www.mdpi.com/1999-4907/7/5/105.
Fick, S.E., Hijmans, R.J., 2017. WorldClim 2: new 1-km spatial resolution climate surfaces for global land areas. Int. J. Climatol. 4315 (May), 4302–4315. http://dx.doi.org/10.1002/joc.5086.
Fischer, R., Bohn, F., Dantas de Paula, M., Dislich, C., Groeneveld, J., Gutiérrez, A.G., Kazmierczak, M., Knapp, N., Lehmann, S., Paulick, S., Pütz, S., Rödig, E., Taubert, F., Köhler, P., Huth, A., 2016. Lessons learned from applying a forest gap model to understand ecosystem and carbon dynamics of complex tropical forests. Ecol. Model. 326, 124–133. http://dx.doi.org/10.1016/j.ecolmodel.2015.11.018.
Frolking, S., Palace, M.W., Clark, D.B., Chambers, J.Q., Shugart, H.H., Hurtt, G.C., 2009. Forest disturbance and recovery: a general review in the context of spaceborne remote sensing of impacts on aboveground biomass and canopy structure. J. Geophys. Res.: Biogeosci. 114 (3). http://dx.doi.org/10.1029/2008JG000911. n/a-n/a.
Gourlet-Fleury, S., Guehl, J.-M., Laroussinie, O., 2004. Ecology and Management of a Neotropical Rainforest: Lessons Drawn from Paracou, a Long-Term Experimental Research Site in French Guiana. Elsevier. http://agritrop.cirad.fr/522004/.
Gourlet-Fleury, S., Blanc, L., Picard, N., Sist, P., Dick, J., Nasi, R., Swaine, M.D., Forni, E., 2005a. Grouping species for predicting mixed tropical forest dynamics: looking for a strategy. Ann. For. Sci. 62 (8), 785–796. http://dx.doi.org/10.1051/forest:2005084.
Gourlet-Fleury, S., Cornu, G., Jésel, S., Dessard, H., Jourget, J.-G., Blanc, L., Picard, N., 2005b. Using models to predict recovery and assess tree species vulnerability in logged tropical forests: a case study from French Guiana. For. Ecol. Manag. 209 (1-2), 69–85. http://dx.doi.org/10.1016/j.foreco.2005.01.010. http://linkinghub.elsevier.com/retrieve/pii/S0378112705000149.
Grau, O., Peñuelas, J., Ferry, B., Freycon, V., Blanc, L., Desprez, M., Baraloto, C., Chave, J., Descroix, L., Dourdain, A., Guitet, S., Janssens, I.A., Sardans, J., Hérault, B., 2017. Nutrient-cycling mechanisms other than the direct absorption from soil may control forest structure and dynamics in poor Amazonian soils. Sci. Rep. 7 (March), 45017. http://dx.doi.org/10.1038/srep45017.
Grimm, V., 2005. Pattern-oriented modeling of agent-based complex systems: lessons from ecology. Science 310 (5750), 987–991. http://dx.doi.org/10.1126/science.1116681. arXiv:1011.1669v3.
Guitet, S., Brunaux, O., Traissac, S., April 2016. Sylviculture pour la production de bois d'oeuvre des forêts du Nord de la Guyane. http://www.onf.fr/guyane/++oid++57df/@@display_media.html.
Hérault, B., Piponiot, C., 2018. Key drivers of ecosystem recovery after disturbance in a neotropical forest. For. Ecosyst. 5 (1), 2. http://dx.doi.org/10.1186/s40663-017-0126-7.
He, L., Chen, J.M., Pan, Y., Birdsey, R., Kattge, J., 2012. Relationships between net primary productivity and forest stand age in U.S. forests. Glob. Biogeochem. Cycles 26 (3), 1–19. http://dx.doi.org/10.1029/2010GB003942.
Hengl, T., de Jesus, J.M., MacMillan, R.A., Batjes, N.H., Heuvelink, G.B.M., Ribeiro, E., Samuel-Rosa, A., Kempen, B., Leenaars, J.G.B., Walsh, M.G., Gonzalez, M.R., 2014. SoilGrids1km – global soil information based on automated mapping. PLOS ONE 9 (8), e105992. http://dx.doi.org/10.1371/journal.pone.0105992.
Holdsworth, A.R., Uhl, C., 1997. Fire in Amazonian selectively logged rain forest and the potential for fire reduction. Ecol. Appl. 7 (2), 713. http://dx.doi.org/10.2307/2269533. http://www.jstor.org/stable/2269533?origin=crossref.
Huth, A., Ditzer, T., 2001. Long-term impacts of logging in a tropical rain forest – a simulation study. For. Ecol. Manag. 142 (1–3), 33–51. http://dx.doi.org/10.1016/S0378-1127(00)00338-8. http://linkinghub.elsevier.com/retrieve/pii/S0378112700003388.
ITTO, 1992. Criteria for the Measurement of Sustainable Forest Management. http://www.itto.int/resource04/.
Johnson, M.O., Galbraith, D., Gloor, M., De Deurwaerder, H., Guimberteau, M., Rammig, A., Thonicke, K., Verbeeck, H., von Randow, C., Monteagudo, A., Phillips, O.L., Brienen, R.J.W., Feldpausch, T.R., Lopez Gonzalez, G., Fauset, S., Quesada, C.A., Christoffersen, B., Ciais, P., Sampaio, G., Kruijt, B., Meir, P., Moorcroft, P., Zhang, K., Alvarez-Davila, E., Alves de Oliveira, A., Amaral, I., Andrade, A., Aragao, L.E.O.C., Araujo-Murakami, A., Arets, E.J.M.M., Arroyo, L., Aymard, G.A., Baraloto, C., Barroso, J., Bonal, D., Boot, R., Camargo, J., Chave, J., Cogollo, A., Cornejo Valverde, F., Lola da Costa, A.C., Di Fiore, A., Ferreira, L., Higuchi, N., Honorio, E.N., Killeen, T.J., Laurance, S.G., Laurance, W.F., Licona, J., Lovejoy, T., Malhi, Y., Marimon, B., Marimon, B.H., Matos, D.C.L., Mendoza, C., Neill, D.A., Pardo, G., Peña-Claros, M., Pitman, N.C.A., Poorter, L., Prieto, A., Ramirez-Angulo, H., Roopsind, A., Rudas, A., Salomao, R.P., Silveira, M., Stropp, J., ter Steege, H., Terborgh, J., Thomas, R., T, M., 2016. Variation in stem mortality rates determines patterns of above-ground biomass in Amazonian forests: implications for dynamic global vegetation models. Glob. Change Biol. 22 (12), 3996–4013. http://dx.doi.org/10.1111/gcb.13315.
Kammesheidt, L., Kohler, P., Huth, A., 2001. Sustainable timber harvesting in Venezuela: a modelling approach. J. Appl. Ecol. 38 (4), 756–770. http://dx.doi.org/10.1046/j.1365-2664.2001.00629.x.
Keller, M., Palace, M., Asner, G.P., Pereira, R., Silva, J.N.M., 2004. Coarse woody debris in undisturbed and logged forests in the eastern Brazilian Amazon. Glob. Change Biol. 10 (5), 784–795. http://dx.doi.org/10.1111/j. 1529-8817.2003.00770.x.
Kiyono, Y., Saito, S., Takahashi, T., Toriyama, J., Awaya, Y., Asai, H., Furuya, N., Ochiai, Y., Inoue, Y., Sato, T., Sophal, C., Sam, P., Tith, B., Ito, E., Siregar, C.A., Matsumoto, M., 2011. Practicalities of non-destructive methodologies in monitoring anthropogenic greenhouse gas emissions from tropical forests under the influence of human intervention. Jpn. Agric. Res. Q. 45 (2), 233–242. http://dx.doi.org/10.6090/jarq.45.233. http://joi.jlc.jst.go.jp/JST.JSTAGE/jarq/45.233?from=CrossRef.
Laporte, N.T., Stabach, J.A., Grosch, R., Lin, T.S., Goetz, S.J., 2007. Expansion of industrial logging in Central Africa. Science 316 (5830), 1451. http://dx.doi.org/10.1126/science.1141057.
Laurance, W.F., Williamson, G.B., 2001. Positive feedbacks among forest fragmentation, drought, and climate change in the Amazon. Conserv. Biol. 15 (6), 1529–1535. http://dx.doi.org/10.1046/j.1523-1739.2001.01093.x.
Lewis, S.L., Edwards, D.P., Galbraith, D., 2015. Increasing human dominance of tropical forests. Science 349 (6250), 827–832. http://dx.doi.org/10.1126/science.aaa9932.
Liang, J., Picard, N., 2013. Matrix model of forest dynamics: an overview and outlook. For. Sci. 59 (3), 359–378. http://dx.doi.org/10.5849/forsci.11-123. https://academic.oup.com/forestscience/article/59/3/359-378/4583685.
Liu, S., Bond-Lamberty, B., Hicke, J.A., Vargas, R., Zhao, S., Chen, J., Edburg, S.L., Hu, Y., Liu, J., McGuire, A.D., Xiao, J., Keane, R., Yuan, W., Tang, J., Luo, Y., Potter, C., Oeding, J., 2011. Simulating the impacts of disturbances on forest carbon cycling in North America: processes, data, models, and challenges. J. Geophys. Res. 116 (4), G00K08. http://dx.doi.org/10.1029/2010JG001585.
Macpherson, A.J., Schulze, M.D., Carter, D.R., Vidal, E., 2010. A model for comparing reduced impact logging with conventional logging for an Eastern Amazonian Forest. For. Ecol. Manag. 260 (11), 2002–2011. http://dx.doi.org/10.1016/j.foreco.2010.08.050. http://linkinghub.elsevier.com/retrieve/pii/S0378112710005219.
Makela, A., Landsberg, J., Ek, A.R., Burk, T.E., Ter-Mikaelian, M., Agren, G.I., Oliver, C.D., Puttonen, P., 2000. Process-based models for forest ecosystem management: current state of the art and challenges for practical implementation. Tree Physiol. 20 (5–6), 289–298. http://dx.doi.org/10.1093/treephys/20. 5-6.289.
Malhi, Y., Gardner, T.A., Goldsmith, G.R., Silman, M.R., Zelazowski, P., 2014. Tropical forests in the Anthropocene. Annu. Rev. Environ. Resour. 39 (1), 125–159. http://dx.doi.org/10.1146/annurev-environ-030713-155141.
Malhi, Y., January 2012. The Productivity, Metabolism and Carbon Cycle of Tropical Forest Vegetation. http://dx.doi.org/10.1111/j. 1365-2745.2011.01916.x.
Maniatis, D., Mollicone, D., 2010. Options for sampling and stratification for national forest inventories to implement REDD+ under the UNFCCC. Carbon Balance Manag. 5 (1), 9. http://dx.doi.org/10.1186/1750-0680-5-9.
Pan, Y., Birdsey, R.A., Phillips, O.L., Jackson, R.B., 2013. The structure, distribution, and biomass of the world's forests. Annu. Rev. Ecol. Evol. Syst. 44 (1), 593–622. http://dx.doi.org/10.1146/annurev-ecolsys-110512-135914.
Pearson, T.R.H., Brown, S., Casarim, F.M., 2014. Carbon emissions from tropical forest degradation caused by logging. Environ. Res. Lett. 034017 (9), 11. http://dx.doi.org/10.1088/1748-9326/9/3/034017.
Pearson, T.R.H., Brown, S., Murray, L., Sidman, G., 2017. Greenhouse gas emissions from tropical forest degradation: an underestimated source. Carbon Balance Manag. 12 (1), 3. http://dx.doi.org/10.1186/s13021-017-0072-2.
Phillips, P., de Azevedo, C., Degen, B., Thompson, I., Silva, J., van Gardingen, P., 2004. An individual-based spatially explicit simulation model for strategic forest management planning in the eastern Amazon. Ecol. Model. 173 (4), 335–354. http://dx.doi.org/10.1016/j.ecolmodel.2003.09.023. http://linkinghub.elsevier.com/retrieve/pii/S030438000300423X.
Picard, N., Magnussen, S., Banak, L.N., Namkosserena, S., Yalibanda, Y., 2010. Permanent sample plots for natural tropical forests: a rationale with special emphasis on Central Africa. Environ. Monit. Assess. 164, 279–295. http://dx.doi.org/10.1007/s10661-009-0892-y.
Piponiot, C., Cabon, A., Descroix, L., Dourdain, A., Mazzei, L., Ouliac, B., Rutishauser, E., Sist, P., Hérault, B., 2016a. A methodological framework to assess the carbon balance of tropical managed forests. Carbon Balance Manag. 11 (1), 15. http://dx.doi.org/10.1186/s13021-016-0056-7.
Piponiot, C., Sist, P., Mazzei, L., Peña-Claros, M., Putz, F.E., Rutishauser, E., Shenkin, A., Ascarrunz, N., de Azevedo, C.P., Baraloto, C., França, M., Guedes, M., Honorio Coronado, E.N., D'Oliveira, M.V., Ruschel, A.R., da Silva, K.E., Doff Sotta, E., de Souza, C.R., Vidal, E., West, T.A., Hérault, B., 2016b. Carbon recovery dynamics following disturbance by selective logging in Amazonian forests. eLife 5 (C). http://dx.doi.org/10.7554/eLife.21394.
Poorter, L., Bongers, F., Aide, T.M., Almeyda Zambrano, A.M., Balvanera, P., Becknell, J.M., Boukili, V., Brancalion, P.H.S., Broadbent, E.N., Chazdon, R.L., Craven, D., de Almeida-Cortez, J.S., Cabral, G.A.L., de Jong, B.H.J., Denslow, J.S., Dent, D.H., DeWalt, S.J., Dupuy, J.M., Durán, S.M., Espírito-Santo, M.M., Fandino, M.C., César, R.G., Hall, J.S., Hernandez-Stefanoni, J.L., Jakovac, C.C., Junqueira, A.B., Kennard, D., Letcher, S.G., Licona, J.-c., Lohbeck, M., Marín-Spiotta, E., Martínez-Ramos, M., Massoca, P., Meave, J.A., Mesquita, R., Mora, F., Muñoz, R., Muscarella, R., Nunes, Y.R.F., Ochoa-Gaona, S., de Oliveira, A.A., Orihuela-Belmonte, E., Peña-Claros, M., Pérez-García, E.A., Piotto, D., Powers, J.S., Rodríguez-Velázquez, J., Romero-Pérez,

I.E., Ruíz, J., Saldarriaga, J.G., Sanchez-Azofeifa, A., Schwartz, N.B., Steininger, M.K., Swenson, N.G., Toledo, M., Uriarte, M., van Breugel, M., van der Wal, H., Velo, M.D.M., 2016. Biomass resilience of neotropical secondary forests. Nature 530 (7589), 211–214. http://dx.doi.org/10.1038/nature16512.

Potapov, P., Hansen, M.C., Laestadius, L., Turubanova, S., Yaroshenko, A., Thies, C., Smith, W., Zhuravleva, I., Komarova, A., Minnemeyer, S., Esipova, E., 2017. The last frontiers of wilderness: tracking loss of intact forest landscapes from 2000 to 2013. Sci. Adv. 3 (1), e1600821. http://dx.doi.org/10.1126/sciadv.1600821.

Putz, F.E., Blate, G.M., Redford, K.H., Fimbel, R., Robinson, J., 2001. Tropical forest management and conservation of biodiversity: an overview. Conserv. Biol. 15 (1), 7–20. http://dx.doi.org/10.1046/j.1523-1739.2001.00018.x. http://www.jstor.org/stable/2641641.

Putz, F.E., Zuidema, P.A., Synnott, T., Peña-Claros, M., Pinard, M.A., Sheil, D., Vanclay, J.K., Sist, P., Gourlet-Fleury, S., Griscom, B., Palmer, J., Zagt, R., 2012. Sustaining conservation values in selectively logged tropical forests: the attained and the attainable. Conserv. Lett. 5 (4), 296–303. http://dx.doi.org/10.1111/j.1755-263X.2012.00242.x.

Rödig, E., Cuntz, M., Rammig, A., Fischer, R., Taubert, F., Huth, A., 2018. The importance of forest structure for carbon fluxes of the Amazon rainforest. Environ. Res. Lett. 13 (5), 054013. http://dx.doi.org/10.1088/1748-9326/aabc61. http://iopscience.iop.org/article/10.1088/1748-9326/aabc61, http://stacks.iop.org/1748-9326/13/i=5/a=054013?key=crossref.0c1e0cf4d5b39bc1cc775f788a94fc7c.

Reis, L.P., Ruschel, A.R., Coelho, A.A., da Luz, A.S., Martins-da Silva, R.C.V., 2010. Avaliaç ao do potencial madeireiro na Floresta Nacional do Tapajós após 28 anos da exploraç ao florestal. Pesqui. Florest. Bras. 30 (64), 265–281. http://dx.doi.org/10.4336/2010.pfb.30.64.265. http://www.cnpf.embrapa.br/pfb/index.php/pfb/article/view/144/138.

Rice, R.E., Gullison, R.E., Reid, J.W., 1997. Can sustainable management save tropical forests? Sci. Am. 276 (4), 44–49. http://dx.doi.org/10.1038/scientificamerican0497-44.

Roopsind, A., Wortel, V., Hanoeman, W., Putz, F.E., 2017. Quantifying uncertainty about forest recovery 32-years after selective logging in Suriname. For. Ecol. Manag. 391, 246–255. http://dx.doi.org/10.1016/j.foreco.2017.02.026. http://linkinghub.elsevier.com/retrieve/pii/S0378112717302256.

Rutishauser, E., Hérault, B., Baraloto, C., Blanc, L., Descroix, L., Sotta, E.D., Ferreira, J., Kanashiro, M., Mazzei, L., D'Oliveira, M.V., de Oliveira, L.C., Peña-Claros, M., Putz, F.E., Ruschel, A.R., Rodney, K., Roopsind, A., Shenkin, A., da Silva, K.E., de Souza, C.R., Toledo, M., Vidal, E., West, T.A., Wortel, V., Sist, P., 2015. Rapid tree carbon stock recovery in managed Amazonian forests. Curr. Biol. 25 (18), R787–R788. http://dx.doi.org/10.1016/j.cub.2015.07.034. http://linkinghub.elsevier.com/retrieve/pii/S0960982215008684.

Rutishauser, E., Hérault, B., Petronelli, P., Sist, P., 2016. Tree height reduction after selective logging in a tropical forest. Biotropica 48 (3), 285–289. http://dx.doi.org/10.1111/btp.12326.

Rykiel, E.J., 1985. Towards a definition of ecological disturbance. Austral Ecol. 10 (3), 361–365. http://dx.doi.org/10.1111/j. 1442-9993.1985.tb00897.x.

Sato, H., Itoh, A., Kohyama, T., 2007. SEIB-DGVM: a new dynamic global vegetation model using a spatially explicit individual-based approach. Ecol. Model. 200 (3–4), 279–307. http://dx.doi.org/10.1016/j.ecolmodel.2006.09.006.

Sebbenn, A.M., Degen, B., Azevedo, V.C.R., Silva, M.B., de Lacerda, A.E.B., Ciampi, A.Y., Kanashiro, M., Carneiro, F.D.S., Thompson, I., Loveless, M.D., 2008. Modelling the long-term impacts of selective logging on genetic diversity and demographic structure of four tropical tree species in the Amazon forest. For. Ecol. Manag. 254 (2), 335–349. http://dx.doi.org/10.1016/j.foreco.2007.08.009.

Sitch, S., Bondeau, A., Cramer, W., Venevsky, S., Analysis, E., 2003. Evaluation of ecosystem dynamics, plant geography and terrestrial carbon cycling in the LPJ dynamic global vegetation model. Glob. Change Biol. 161–185.

Stocker, T., 2014. Climate Change 2013 – The Physical Science Basis. Cambridge University Press, Cambridge. http://dx.doi.org/10.1017/CBO9781107415324. arXiv:1011.1669v3.

Swaine, M.D., Lieberman, D., Putz, F.E., 1987. The dynamics of tree populations in tropical forest: a review. J. Trop. Ecol. 3 (04), 359–366. http://dx.doi.org/10.1017/S0266467400002339.

ter Steege, H., Pitman, N.C.A., Sabatier, D., Baraloto, C., Salomao, R.P., Guevara, J.E., Phillips, O.L., Castilho, C.V., Magnusson, W.E., Molino, J.-F., Monteagudo, A., Nunez Vargas, P., Montero, J.C., Feldpausch, T.R., Coronado, E.N.H., Killeen, T.J., Mostacedo, B., Vasquez, R., Assis, R.L., Terborgh, J., Wittmann, F., Andrade, A., Laurance, W.F., Laurance, S.G.W., Marimon, B.S., Marimon, B.-H., Guimaraes Vieira, I.C., Amaral, I.L., Brienen, R., Castellanos, H., Cardenas Lopez, D., Duivenvoorden, J.F., Mogollon, H.F., Matos, F.D.D.A., Davila, N., Garcia-Villacorta, R., Stevenson Diaz, P.R., Costa, F., Emilio, T., Levis, C., Schietti, J., Souza, P., Alonso, A., Dallmeier, F., Montoya, A.J.D., Fernandez Piedade, M.T., Araujo-Murakami, A., Arroyo, L., Gribel, R., Fine, P.V.A., Peres, C.A., Toledo, M., Aymard, G.A., Baker, C.T.R., Ceron, C., Engel, J., Henkel, T.W., Maas, P., Petronelli, P., Stropp, J., Zartman, C.E., Daly, D., Neill, D., Silveira, M., Paredes, M.R., Chave, J., Lima Filho, D.D.A.P., 2013. Hyperdominance in the Amazonian Tree Flora. Science 342 (6156), 1243092. http://dx.doi.org/10.1126/science.1243092.

Thompson, J.N., Reichman, O.J., Morin, P.J., Polis, G.A., Power, M.E., Sterner, R.W., Couch, C.A., Gough, L., Holt, R., Hooper, D.U., Keesing, F., Lovell, C.R., Milne, B.T., Molles, M.C., Roberts, D.W., Strauss, S.Y., 2001. Frontiers of ecology. BioScience 51 (1), 15–24. http://dx.doi.org/10.1641/0006-3568(2001)051[0015:foe]2.0.co;2.

Tyukavina, A., Hansen, M.C., Potapov, P.V., Krylov, A.M., Goetz, S.J., 2016. Pan-tropical hinterland forests: mapping minimally disturbed forests. Glob. Ecol. Biogeogr. 25 (2), 151–163. http://dx.doi.org/10.1111/geb.12394.

Valle, D., Phillips, P., Vidal, E., Schulze, M., Grogan, J., Sales, M., van Gardingen, P., 2007. Adaptation of a spatially explicit individual tree-based growth and yield model and long-term comparison between reduced-impact and conventional logging in eastern Amazonia, Brazil. For. Ecol. Manag. 243 (2–3), 187–198. http://dx.doi.org/10.1016/j.foreco.2007.02.023. http://linkinghub.elsevier.com/retrieve/pii/S0378112707001417.

Volkova, L., Roxburgh, S.H., Weston, C.J., Benyon, R.G., Sullivan, A.L., Polglase, P.J., 2018. Importance of disturbance history on net primary productivity in the world's most productive forests and implications for the global carbon cycle. Glob. Change Biol. 0–2. http://dx.doi.org/10.1111/gcb.14309.

Wagner, F., Hérault, B., Stahl, C., Bonal, D., Rossi, V., 2011. Modeling water availability for trees in tropical forests. Agric. For. Meteorol. 151 (9), 1202–1213. http://dx.doi.org/10.1016/j.agrformet.2011.04.012. http://linkinghub.elsevier.com/retrieve/pii/S0168192311001419.

Walters, C., 1999. Ecospace: prediction of mesoscale spatial patterns in trophic relationships of exploited ecosystems, with emphasis on the impacts of marine protected areas. Ecosystems 2 (6), 539–554. http://dx.doi.org/10.1007/s100219900101.